Centrifuge Model Test and FEM Analysis of Dynamic Interactive Behavior between Embankments and Installed Culverts in Multiarch Culvert Embankments

AUTHOR(S):

Sawamura, Yasuo; Kishida, Kiyoshi; Kimura, Makoto

Centrifuge model test and its FEM analysis of dynamic interactive behavior between embankment and installed culverts in multi-arch culvert embankment

Yasuo Sawamura[1], Kiyoshi Kishida[2] and Makoto Kimura[3]

Keyword
centrifuge model test, FEM analysis, dynamic interaction between soil and structure, embankment, precast arch culvert,

ABSTRACT

A multi-arch culvert embankment is a new type of filling structure for which several precast arch culverts are installed continuously in the direction of the road extension. The key points in the design are to estimate the practical optimal spacing between installed arch culverts and to clarify the interactive seismic behavior of the filling material and the culvert structure. In the present study, firstly, dynamic centrifuge model tests and a numerical analysis are carried out to clarify the basal earthquake behavior of this structure and verify the numerical approach. Then, the full-scale numerical analysis has been executed to investigate the influence of spacing between multi-arch culverts and mechanical behavior under seismic conditions. From the results, it is confirmed that when the unit spacing is narrow, the whole rigidity of the ground and the arch culvert increases relatively. This is because the volume in the fill part, where the rigidity is small, decreases comparatively. Hence, the section force and the deformation are controlled.

INTRODUCTION

When an arterial high-standard highway is built, it is necessary to construct the fill or the elevated bridge to overpass other roads and railways. Most of the time, however, the fill structure acts as a wall that partitions an area. Unlike an elevated bridge, that does not partition an area into two, fill structures often create a partition, thereby obstructing the free flow of the wind and denying people direct access. Recently, multi-arch culvert embankments (Fig. 1) of continuously arranged precast arch culverts in the direction of the road extension are proposed as a solution to such problems. The shape of the embankment is close to that of a bridge structure, due to the void space of the precast arch culverts, and it is more open than with the general fill method. Continuous arch culverts make the structure blend in well with the environment and beautify the scenery. The reuse of the removed soil from the cut ground is also possible,

[1]Doctoral student, Department of Civil and Earth Resources Engineering, Kyoto University, C1, Kyoto Daigaku Katsura, Nishikyo, Kyoto, Japan.
[2]Associate Professor, Department of Urban Management, Kyoto University, C1, Kyoto Daigaku Katsura, Nishikyo, Kyoto, Japan.
[3]Professor, Department of Civil and Earth Resources Engineering, Kyoto University, C1, Kyoto Daigaku Katsura, Nishikyo, Kyoto, Japan.

therefore being more economical than an elevated bridge. It is expected that the demand for this new type of structure will increase in the future from an economic point of view.

The design of traditional culvert structures in Japan has not considered seismic stability, because such structures have not suffered terrible damage in past earthquakes. Even now, therefore, it is thought that earthquake stability need not be considered for the range in application of traditional culverts. Table 1 shows the range in application of traditional culverts. For each type of culvert, the range in overburden and scale section has been determined. In addition to the conditions defined on the table, the following seven requirements should be met in order to apply the design to traditional culverts.

1) Back-filling made from soil
2) Within 10% of the longitudinal gradient
3) No hinges in the main body structure
4) Not be a multiple-string structure according to an inside pillar
5) Set up alone
6) Supported with a spread foundation
7) Overburden with a thickness over 50 cm

In multi-arch culvert embankments, as several arch culverts are lined consecutively, the 5th condition is not fulfilled. Moreover, precast arch culverts, which are used in multi-arch culvert embankments, have two hinges in the main body structure, and thus, the 3rd condition is not fulfilled either. For single precast arch culverts, various research works on topics such as the earth pressure acting on the culvert during the laying process (Adachi et al., 2001), the relation of the bearing capacity and the embedded depth of the foundation type (Murakami et al., 2008), the performance assessment of a precast-concrete arch bridge system (Zoghi et al., 2006), have been carried out.

With regard to earthquake resistance of single arch culvert, various experiments and numerical analyses (Byrne et al., 1994; Wood and Jenkins, 2000; Arai et al., 2011) have been carried out and earthquake-proof verification was performed. Moreover, it is confirmed that culverts can maintain stability regardless of the ground displacement, like the one observed by the Great Hanshin Earthquake in 1995. Since only a numerical analysis was carried out to study the earthquake resistance of multi-arch culvert embankments, however, the research cannot be said to have been sufficient.

A couple of research works have been done to investigate the earthquake-proof stability of multi-arch culvert embankments through numerical analyses. Through a dynamic finite element method (FEM) analysis, Hwang et al. (2006, 2007) investigated the influence of the spacing between multi-arch culverts and concluded that the increase in ground stress and volumetric strain was constricted when the spacing between arch culverts was close. In seismically active countries, like Japan, an investigation of the

earthquake-proof stability is necessary and indispensable. Therefore, in addition to a numerical analysis, an experimental study is also deemed important.

It is thought that the greatest factor affecting the earthquake resistance of multi-arch culvert embankments is the spacing between consecutive arch culverts installed in the embankment.

When the unit spacing is narrow, it is thought that there is a possible increase in the interaction of the arch culverts, because the volume of the ground between units becomes smaller and the response of an arch culvert and its surrounding soil increases.

In the present study, firstly, dynamic centrifuge model tests and a FEM analysis are carried out to clarify the basal earthquake behavior of this structure and verify the numerical approach. In the experiment, however, two units of arch culverts were modeled due to the restriction of soil chamber. Hence the full-scale numerical analysis which removed the boundary effect has been executed to investigate the influence of spacing between multi-arch culverts and mechanical behavior under seismic conditions.

CENTRIFUGE MODEL TESTS

Experimental set-up

Centrifuge model tests were performed under a gravitational acceleration of 50 G. A soil chamber, 450 mm long, 300 mm deep and 150 mm wide, with a transparent front window, was used for the tests. Fig. 2 shows the set-up of the culvert models and the arrangement of the sensors and the strain gauges. In this experiment, the acceleration of the ground at the center of the unit, the earth pressure of the ground subsurface, the surface displacement and the strain of the culvert model were measured. The experimental model represented a 5.0-m fill to be constructed on a 7.5-m-thick sandy ground. In the *in situ* construction, several precast arch culverts are usually set up continuously. However, in this experiment, two units of arch culverts were used due to experimental restrictions. A light fill material can be used, as shown in Fig. 1, to reduce the earth pressure during earthquakes and to alleviate the load of the lower ground. This results in the unit spacing being smaller than in cases where an ordinary fill material is used. The difference in the dynamic behavior by unit spacing was examined in this study using a sandy fill ground.

Arch culverts

The arch culverts were 4.3 m in height and 6.4 m in width. The overburden soil above the arch culverts was 0.7 m. The dimensions of the arch culvert model are shown in Fig. 3. The arch culvert model used in the experiment was made from mortar (the combined ratio of silica sand No. 6, high early strength cement and water was 2: 1: 0.65). The arch culvert model was cured in water for 28 days after casting. The model was then dried in air for 24 hours and, after that, oven dried for another 24 hours. Table 2 shows the material constants of the arch culvert model. *In situ* precast arch culverts were made by joining several

precast sections, and their joints were connected using pre-stressed concrete wire. The joint stiffness is somewhere between rigid and hinged. However, the arch culvert model in this study was made as an all-in-one design structure in order to make a simple model. Arai et al. (2011) carried out centrifuge model tests to compare the two different structures of the shoulder part. In this experiment, two culvert models, one culvert with a hinged shoulder frame and the other with a rigidly connected frame, were used. From the experimental results, it is confirmed that the burden rate of the foot part in the culvert with the rigidly connected frame is smaller than that of the culvert with the hinged shoulder, because the shoulder part might also resist the seismic force. Since this experiment was conducted under plane distortion conditions, it is important to reduce the friction with the soil chamber. The arch culvert model was divided into three parts in the depth direction, and sponge tape was thinly stuck between the culvert models and between the wall and the models in order to reduce friction.

In this experiment, the strain of the arch culverts was measured to calculate the bending moment and the axial force generated on an arch culvert. A strain gauge was stuck on both feet parts, both shoulder parts and the top part of the middle of the divided three pieces. The arch culvert model is shown in Fig. 4.

Embankment and ground

Both the foundation ground and the filling were made from dry Toyoura sand using a sand hopper. The falling height of the sand was adjusted in such a way that a relative density of 85% was achieved. Table 3 shows the properties of Toyoura sand. The reason for making a dense sandy ground is that when the arch culverts are set up directly on the ground without ground improvement, the N value of the foundation ground is defined as 15 or more in the design manual. The design manual also describes the degree of compaction as being not less than 92% in many cases of filling construction.

Input wave and experimental cases

The wave pulse of the prototype, 1 Hz, was input by controlling the displacement of the vibration table. Fig. 5 shows the time history of the input wave. The aim of the experiment is to investigate the influence of the spacing between installed arch culverts on the earthquake-proof stability of the structure. Unit spacing L, between the precast arches, were expressed as a function of culvert height H. Three spacing of 0.5 H, 1.0 H and 1.5 H were adopted in the experiment. The results from these three patterns were compared to a case of fill only without precast arch culverts. Fig. 6 shows the experiment cases.

EXPERIMENTAL RESULTS

Acceleration at center of unit

Fig. 7 shows the time history of the acceleration in the vicinity of the ground level for the case with only fill and without arch culverts (Case-0) and for the case where the spacing between installed arch culverts

was L=1.0 H (Case-3). From this figure, it can be seen that both cases produced similar phases and maximum acceleration regardless of the presence or absence of arch culverts. In Fig. 8, the maximum accelerations from the five acceleration measured points obtained from all the experimental cases are plotted. The maximum acceleration at a distance between 12 m (Acc-5) and 9 m (Acc-4) below the height of the fill for Case-0 was seen to be constant. From a depth of 9 m to the surface of the fill, the maximum acceleration is amplified. In cases where arch culverts were incorporated, only Case-4, where the unit spacing was the widest, showed a similar pattern to that observed in Case-0. This is due to the fact that the unit spacing in Case-4 is so wide that the arch culverts had few influence on the ground at the center of the culverts. Therefore, when the unit spacing is wide enough, it can be concluded that the behavior of the soil between the arches is similar to the case in which there are no culverts. In all cases, the influence of the installation spacing on the fill between the arch culverts was similar.

Bending moments

When the stability of a concrete structure against earthquakes is evaluated, the point that is noteworthy is the generation of excessive bending moments. Fig. 9 shows the distribution of bending moments generated in the arch culverts. A positive bending moment is defined for the case where tension is generated inside the arch culvert. The dotted line in the figure shows a bending crack generation moment. The following four states, (a) the initial state, (b) when the maximum bending moment is generated at the right foot, (c) when the maximum bending moment is generated at the left foot and (d) the residual status, are shown in the figure. Bending moments are hardly generated in the shoulders at the initial state, showing that the arch culverts may have a support mechanism through the axial force. Furthermore, it can be seen that bending moments are hardly generated in the top part because of the shallow overburden under this experimental condition. When arch culverts bend, as a result of seismic force, a large bending moment is generated at the foot where hitching occurs. In this experiment, regardless of the unit spacing the bending moment did not reach the crack generation moment in any of the cases when the response acceleration spectrum in the vicinity of the ground level was about 5.5 m/sec^2. It can also be seen from Fig. 9 that the initial and the residual bending moments are the same level, though the residual value became little larger than the initial value at feet near the soil chamber. This implies that the deformation of the ground and the arch culvert from the initial state to the residual state is small. Moreover, the increment of bending moment from the initial is almost same value for all cases in each states and no significant change was observed as a result of unit spacing.

FEM ANALYSIS Of EXPERIMENT

Model of simulation

In this study, 2-D elasto-plasticity FEM analysis was performed using a program named as `DBLEAVES'

(Ye et al., 2007). This FEM code was developed based on DGPILE-3D (Kimura and Zhang, 2000), which is developed in order to investigate the static and dynamic interaction between soil and pile foundation. These FEM codes are used for not only pile foundation (Danno and Kimura, 2009; Zhang et al., 2010) but also tunnel (Cui et al., 2010) and underground structure (Xia et al., 2010).

This analysis was done for the experimental cases. In the experiment, the narrowest unit spacing that could be achieved was L=0.50 H, due to experimental restrictions in the analysis of the case with L=0.25 H (Case-1). The analytical mesh and the boundary conditions are as shown in Fig. 10. Since a rigid soil chamber was used in the experiment, the analytical domain was made to be the same size as the soil chamber with both sides horizontally restrained.

The input ground motions used in this analysis is the time history of acceleration measured by Case-3 of the experiment shown in Fig. 5 (b). In the dynamic analysis, viscous damping is adopted and the direct integration method of Newmark-β (β=1/4, γ=1/2) is used and the time interval of calculation is 0.001 seconds.

Modeling of ground

The constitutive model for the Toyoura sand is the subloading t_{ij} model (Nakai and Hinokio, 2004). This model was proposed based on the concept of SMP (Spatially Mobilized Plane), in which the influence of the intermediate principal stress can be properly evaluated. Furthermore, this model can describe the dependence of the direction of the plastic flow on the stress paths, density and confining pressure on the deformation and strength of the soil. The properties of Toyoura sand are given in Table 4. Fig. 11 shows the element simulation results of Toyoura sand. Because the rigid soil chamber was used in the experiments, it has a high degree of potential for damping ratio of soil being higher than in-situ construction. Although the research on damping ratio of soils during centrifuge tests was carried out by Brennan et al. (2005), it is difficult to determine it correctly through experiment. Therefore, the pre-analysis in which the damping coefficient of the ground was changing parameter (h=5, 10, 20, 30, 40 and 50%) were conducted preliminarily and then the ratio was dictated as 30%.

Modeling of structure

While modeling the structure, the nonlinearity of the concrete was also considered. For culvert concrete, the nonlinear moment-curvature relation was simulated using the AFD (Axial Force Dependent) model (Zhang and Kimura, 2002). This model introduces the concept of multi-spring model and fiber model (Lai et al., 1984; Li and Kubo, 1999) into the finite element method by proposing a new weak form of equilibrium equation for a beam, which satisfies the compatibility of the deformation. Therefore, the axial-force dependency according to the variable axial force of the structure can be considered by using this model.

Moreover, the interface element was arranged on the boundary division of the culverts and the ground to represent the influence of friction. The parameters of the interface element, as shown in Table 5, were defined from box shear tests between Toyoura sand and the concrete element. And the damping coefficient of the arch culvert is assumed as 2%.

ANALYTICAL RESULTS Of EXPERIMENT

Comparison with centrifuge model tests in Case-3

Fig. 12 shows the time history of the acceleration and the Fourier spectrum of Acc-1 and Acc-2 for Case-3. The acceleration obtained from the analysis tends to become small in the vicinity of the maximum and the minimum values compared with the acceleration obtained from the experiment. However, the analysis precisely replicates the experiment as a whole. In addition, from the figure of the Fourier spectrum, it is seen to almost perfectly reproduce the acceleration.

The initial distributions of bending moments and axial force in Case-3 are shown in Fig. 13. The circle and square lines represent the experimental and the analytical values, respectively. Firstly, take a look at the bending moment. The bending moment is large at the feet and small in the shoulders and the top part at the initial state. These results are consistent with the experimental values as well. Then, in the initial distribution of axial force, although a large axial force has occurred at the feet in both the experiment and the analysis, the experimental values are smaller in the shoulders and the top part at the left arch culvert. It is because dry sand was used under shallow overburden condition in the experiment, confined pressure was small and influence of sand displacing along with the arch came out greatly during increment of centrifugal force. However, compared with Case-3, the experimental values in the shoulders and the top part in Case-2 and Case-4 were large, and the difference between the experimental values and the analytical values was smaller.

The time histories of the bending moments and the axial force in each position of the left arch culvert in Case-3 are shown in Fig. 14. In the bending moments, it is thought that the analytical results reproduce the experimental results comparatively well, although the behavior after 3 seconds becomes a little large. In the time history of the axial force, although the initial value is different from the start in the shoulders and the top part, as referred to above, it can be seen that the tendency of the experiment is reproduced.

Comparison with centrifuge model tests in all cases

Fig. 15 shows the distribution of bending moments in FEM analysis. The following three states, (a) the initial state, (b) when the maximum bending moment is generated at the right foot and (c) the residual status, are shown in the figure. At the initial state, bending moment at the right foot on left-side arch culvert is slightly-great in Cases with wide unit spacing. This is because the volume of fill part at the unit spacing increases comparatively, the weight of the ground increased. On the other hand, bending moment

at the left foot on left-side arch culvert increases in Case with narrow unit spacing because of the increment of distance from the soil chamber. When maximum bending moment occurring at the right foot, bending moment distribution differs by culvert on either side. When the arch culvert inclines to the left, it is thought that left-hand side arch culvert is strongly restricted by the soil chamber. In left-hand side arch culvert, therefore, it can de seen that bending moment distribution differe between cases at the left sholder and left corner of intersection. At the left sholder, the case where a unit spacing is large, in other words, the case where distance from the soil chamber is near, the bending moment becomes small. Moreover, since displacement was controlled by the soil chamber, in the case where distance with the soil chamber is small, the large bending moment has occurred at the left corner of intersection regardless of the time in which sectional force become small originally at these area. Meanwhile the bending moment at right corner become larger as unit spacing increse.

Then, it focuses to the right-hand side arch culvert at this moment. Here, since right-hand side arch culvert is hardly subjected to the influence of the soil chamber, it is considered that the influence by a unit spacing somewhat appropriately. At the part from the left shoulder to left foot, imperceptibly large bending moment is generated in the case with wide unit spacing. This could be the result of the arch culverts shaking greatly, because the volume in the fill part, where the rigidity is small, increases comparatively when the unit spacing is wide.

In order to explain this behavior, the lateral deformation at the center of the units, for all analytical cases incorporating arch culverts, is shown in Fig. 16. From the figure, it is clearly understood that the lateral deformation becomes large when the unit spacing broadens.

However, well-marked difference of bending moment between cases is only at the corner of intersection, and difference at other parts is several percent. It can be concluded, therefore, that the difference in bending moments was not able to be confirmed accurately through the experimental study.

After shaking, the residual value became little larger than the initial value at corners of intersection near the soil chamber in common with experiment.

Fig. 17 shows the time history of the vertical earth pressure ratio on the lower foundation of the arch culvert installed on the right-hand side. In this paper, the vertical earth pressure ratio is defined as the measurement value normalized by the initial value. Compared with experimental values, the analytical values reach a peak belatedly, but the analysis reproduces the tendency for the vertical earth pressure ratio become large with wide unit spacing and the behavior after 3 seconds. The maximum vertical earth pressure ratio of P-1 and P-2 are shown in Fig. 18. P-1 and P-2 in Fig. 18 show that the maximum vertical earth pressure ratio becomes large as the unit spacing becomes large. In order to check the distribution of earth pressure for the culvert, the earth pressure of normal direction which acts on the boundary portions of the ground and the right-hand side culvert when the P-1reaches the maximum were shown in Fig. 19. From the figure, it can be seen that the large earth pressure is generated at the culvert’s right and left side

in the case where a unit spacing is large, hence large earthpressure has occurred in the left end part of invert, and vertical earth pressure ratio of P-1 enlarged.

Based on the above results, the experimental study could be simulated accordingly in the present study by using a constitutive model for the ground and the arch culverts.

FULL-SCALE NUMERICAL ANALYSIS

Model of simulation

In the experiment and its FEM analysis, two units of arch culverts were modeled due to the restriction of soil chamber. However, this model is expected the boundary effects from the wall. Hence the full-scale numerical analysis which removed the boundary effect has been executed to investigate the influence of spacing between multi-arch culverts and mechanical behavior under seismic conditions.

The analytical object and numerical modeling are same as centrifuge model test and its FEM analysis except for the damping coefficient of the ground. In the full-scale numerical analysis, the damping coefficient of the ground is assumed as 5%. Unit interval L between the precast arches was expressed as a function of the culvert height H. Results of the case with consecutive arch culverts were compared to cases of single arch culvert setting alone. The examination cases are shown in Table 6. In the cases of multi-arch culverts embankment, since several precast arch culverts are set up continuously in the in-situ construction, 1 unit of arch culvert was modeled and both sides of analytical domain were configured equal displacement condition of horizontal and vertical direction. Moreover, the boundary on the bottom area is fixed on all directions. On the other hand, in the case of single arch culvert, the width of analytical domain is wide enough (100 m) and boundary condition is same as other cases. The analysis mesh of Case-1and 4 and boundary condition were as shown in Fig. 20.

Results of simulation

Fig. 21 shows the distribution of maximum bending moment occurring at right foot, and Fig. 22 shows the initial and maximum bending moment at the right foot. From these figures, it can be seen that the influence of the installation spacing on the fill between arch culverts was remarkable in the right foot and the right end part of invert. The maximum bending moment in Case-4 increased by about 13 % compared with Case-1. Moreover, when unit spacing is wide, large bending moment is already generated in the initial state because of the self-weight of the surrounding soil.

Fig. 23 shows the horizontal displacement of soil around arch culvert when the maximum bending moment is generated at right foot. In this figure, two lines which is left and right side of arch culvert are pick up. In Case-1, the difference of displacement hardly occurs. It is because arch culvert and surrounding soil behave monolithically. On the other hand, it can be seen that the difference of displacement has occurred on the left-line and right-line in other cases. The difference of displacement is

large at the boundary between fill and foundation ground and ground surface. Moreover, when unit spacing is wide, the difference of displacement increases and comes to the behavior of Case-single.

Fig. 24 shows the earth pressure distribution of normal direction which acts on the boundary portions of the ground and arch culvert when maximum bending moment is generated at right foot. When the arch culvert bends to the left, as a result of seismic force, it turns out that a large earth pressure acts on the right-hand side of arch culvert. Compared all cases, earth pressure also becomes large as a unit spacing become large. This could be ascribable to the difference of horizontal displacement of soil around arch culvert as shown in Fig. 23. On the other hand, near the top part of the arch culvert, a difference is not seen between cases.

Fig. 25 shows the variation of axial force with bending moment at the right foot. During earthquake, the bending moment for all cases increase accompanied by increase in axial force. When all cases are compared, the more unit spacing is wide, the more both axial force and bending moment increase, and there are few differences between Case-4 and Case-Single. It can be concluded that arch culverts and surround soil shake greatly because the volume in the fill part where the rigidity is comparatively small increases when unit interval is wide.

Fig. 26 shows the settlement of ground surface and Fig. 27 shows the grade of settlement. The grade of settlement is defined as unequal settlement ΔS divided by distance from the top part of arch culvert to the center of the unit l. At the top part of arch culvert, settlement is almost same in all the cases. However, when the installation spacing is wide, the amount of the subsidence at the center of the unit becomes large. It is because that the volume in the fill part where the weight is comparatively large increases when unit spacing is wide. Therefore, Unequal settlement becomes large. But the grade of settlement is only 0.03% in Case-4 and it does not become a serious traffic hindrance. Furthermore, surface geometry is continuity and local discontinuous subsidence like the case of box culvert does not occur.

CONCLUSION

In this study, firstly, dynamic centrifuge model tests and a FEM analysis are carried out to clarify the basal earthquake behavior of this structure and verify the numerical analytical approach. In the experiment, however, two units of arch culverts were modeled due to the restriction of soil chamber. Hence the full-scale numerical analysis which removed the boundary effect has been executed to investigate the influence of spacing between multi-arch culverts and mechanical behavior under seismic conditions. The following conclusions can be drawn from the results of this study:

1) When earthquake-proof stability of culvert is examined, the generation of bending moment at the foot is especially important, and the influence of the installation interval on the fill between arch culverts was remarkable at the foot.
2) In case with wide unit spacing, large maximum bending moment is generated compared with the case

with narrow unit spacing.

3) For case with wide unit spacing, bending moment increases accompanied by an increase in the axial force. It is thought that arch culverts shake widely because the volume in the fill part where the rigidity is small increases comparatively when the unit spacing is wide.

4) When the installation spacing is wide, the amount of the subsidence at the center of the unit becomes large, hence unequal settlement becomes large. However, the grade of settlement is very small and it does not become a serious traffic hindrance.

REFERENCES

Adachi, T., Kimura, M., Kishida, K. and Samejima, R. (2001). ‘‘Model Tests on The Earth Pressure Acting on The Precast Tunnels.’’ *Proceedings of the Regional Conference on Geotechnical Aspects of Underground Construction in Soft Ground (SHANGHAI2001)* , Shanghai, China: 151–156.

Arai, T., Sawamura, Y., Kishida, K. and Kimura, M. (2011). ‘‘Behavior of Culvert Embankment in Dynamic Centrifuge Model Test.’’ *Proceedings of the 24th KKCNN Symposium on Civil Engineering*, Awaji, Japan, 353-356.

Brennan, A., Thusyanthan, N., and Madabhushi, S. (2005). ”Evaluation of Shear Modulus and Damping in Dynamic Centrifuge Tests.” *J. Geotech. Geoenviron. Eng.*, 131(12), 1488–1497.

Byrne, P. M., Anderson, D. L. and Jitno, H. (1994). ‘‘Seismic Analysis of Large Buried culvert Structures.’’ *Transportation Research Record* No. 1541, 133-139.

Cui, Y. Kishida, K. and Kimura, M. (2010). ‘‘Analytical study on the control of ground subsidence arising from the phenomenon of accompanied settlement using footing reinforcement pile.’’ *Deep and Underground Excavation, ASCE Geotechnical Special Publication*, 307-312.

Danno, K. and Kimura, M. (2009). ‘‘Evaluation of long-term displacements of pile foundation using coupled fem and centrifuge model test.’’ *Soils and Foundations*, 49(6), 941-958.

Hwang, J. H., Kikumoto, M., Kishida, K. and Kimura, M. (2006) ‘‘Dynamic Stability of Multi-Arch Culvert Tunnel Using 3-D FEM.’’ *Proceedings of the World Tunnel Congress and 32nd ITA Assembly*, Seoul, Korea, 22–27.

Hwang, J. H., Kishida, K. and Kimura, M. (2007) ‘‘Numerical Study for Interaction between Structure and Ground of Multi-Arch Culverts with Filling Embankment under Seismic Condition.’’ *Proceedings of the 20th KKCNN Symposium on Civil Engineering*, Jeju, Korea, 346-349.

Kimura, M. and Zhang, F. (2000). ‘‘Seismic evaluations of pile foundations with three different methods based on three-dimensional elasto-plastic finite element analysis.’’ *Soils and Foundations*, 40(5), 113-132.

Lai, S-S., Will, G. T. and Otani, S. (1984). ‘‘Model for inelastic biaxial bending of concrete member.’’ *Journal of Structural Engineering, ASCE*, 110 (11), 2568-1584.

Li, K. N. and Kubo, T. (1999). ‘‘Analysis of circular RC member in MS/fiber model.’’ *Summaries of Technical Papers of Annual Meeting*, Hiroshima St., II, AIJ.

Murakami, Y., Kishida, K., Kimura, M., Iwasaki, T. and Kodaka, T. (2008). ‘‘Estimation of Ultimate Bearing Capacity of Foundation by Pre-cast Arch Culvert.’’ *JSCE JOURNAL*, 64(2), 282-293. (in Japanese)

Nakai, T. and Hinokio, M. (2004). ‘‘A Simple Elastoplastic Model for Normally and Over Consolidated Soils with Unified Material Parameters.’’ *Soils and Foundations*, 44(2), 53-70.

Wood, J. H. and Jenkins, D. A. (2000). ‘‘Seismic analysis of buried arch structures.’’ *12th World Conference of Earthquake Engineering*, Oakland, New Zealand, No.0798.

Xia, Z. f., Ye, G. L., Wang, J.H., Ye, B and Zhang, F. (2010). ‘‘Numerical analysis on the influence of thickness of liquefiable soil on seismic response of underground structure.’’ *Journal of Shanghai Jiaotong University (Science)*, 15(3).

Ye, B., Ye, G. L., Zhang, F. and Yashima, A. (2007). ‘‘Experiment and numerical simulation of repeated lipuefaction-consolidation of sand.’’ *Soils and Foundations*, 47(3), 547-558.

Zhang, F., Jin, Y., Bao, X., Kondo, Y. and Nakamura, K. (2010). ‘‘Soil-water coupling finite element analysis on seismic enhancement effect of group-pile foundation with ground improvement.’’ *IOP Conference Series Materials Science and Engineering*, 10(1).

Zhang, F. and Kimura, M. (2002). ‘‘Numerical Prediction of the Dynamic Behaviors of an RC Group-Pile Foundation.’’ *Soils and Foundations*, 42(3), 77-92.

Zoghi, M. and Farhey, D. (2006). ”Performance Assessment of a Precast-Concrete, Buried, Small Arch Bridge.” *J. Perform. Constr. Facil.*, 20(3), 244–252.

Table 1. Range in application of traditional culverts

Type of culvert		Overburden [m]	Scale of section [m]
Box culvert	Cast-in-place	0.5～20	Width of inner space B： within 6.5 Height of inner space H： within 5.0
	Precast section	0.5～6	Width of inner space B： within 5 Height of inner space H： within 2.5
Gate culvert		0.5～10	Width of inner space B： within 8
Arch culvert	Cast-in-place	Above 10	Width of inner space B： within 8
	Precast section	0.5～14	Width of inner space B： within 3 Height of inner space H： within 3.2

Table 2. Material constants of arch culvert model

Young's modulus [kN/m^2]	2.07×10^7
Compressive strength [kN/m^2]	4.92×10^4
Bending strength [kN/m^2]	1.17×10^4
Tensile strength [kN/m^2]	5.76×10^3
Poisson's ratio	0.18

Table 3. Properties of Toyoura Sand

Specific gravity	2.64
Average grain diameter [mm]	0.2
Maximum void ratio	0.975
Minimum void ratio	0.585
Relative density [%]	85

Table 4. Parameters of Toyoura sand

Unit weight γ [kN/m^3]	15.76
Principal stress ratio at critical state R_{CS}	3.2
Poisson's ratio ν	0.333
Coefficiennt of earth pressure at rest K_0	0.5
Void ratio e_0	0.64
β（stress-dilatancy）	2
a（ANN） parameter	500
Compression index λ	0.07

Swelling index κ	0.0045
Damping coffecient h	0.3

Table 5. Parameters of interface element

Shear stiffness K_s [kN/m^2]	1.55×10^5
Normal stiffness K_n [kN/m^2] (Assumed)	1.00×10^5
Cohesion C [kN/m^2]	5.0
Internal friction angle ϕ [deg]	28.0

Table 6. Examination cases

Case	Unit interval (Number of node: N, Number of element: E)
Case-1	L=0.25H (N: 934, E: 786)
Case-2	L=0.50H (N: 1054, E: 902)
Case-3	L=1.00H (N: 1294, E: 1134)
Case-4	L=1.50H (N: 1534, E: 1366)
Case-Single	∞ (N: 3574 , E: 3338)

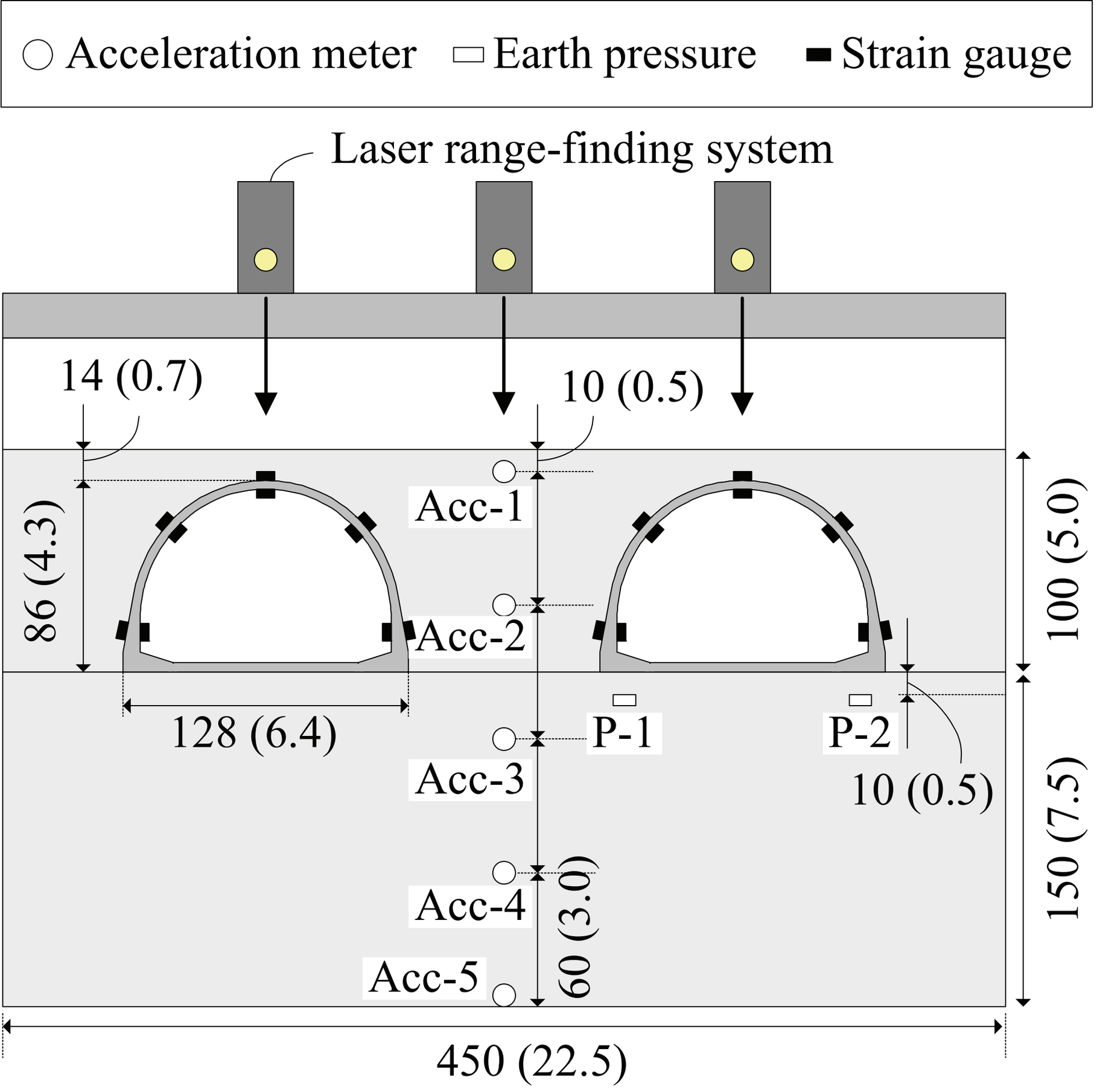

Unit: mm (in parenthesis, it is a prototype size)

Fig. 2

Fig. 3

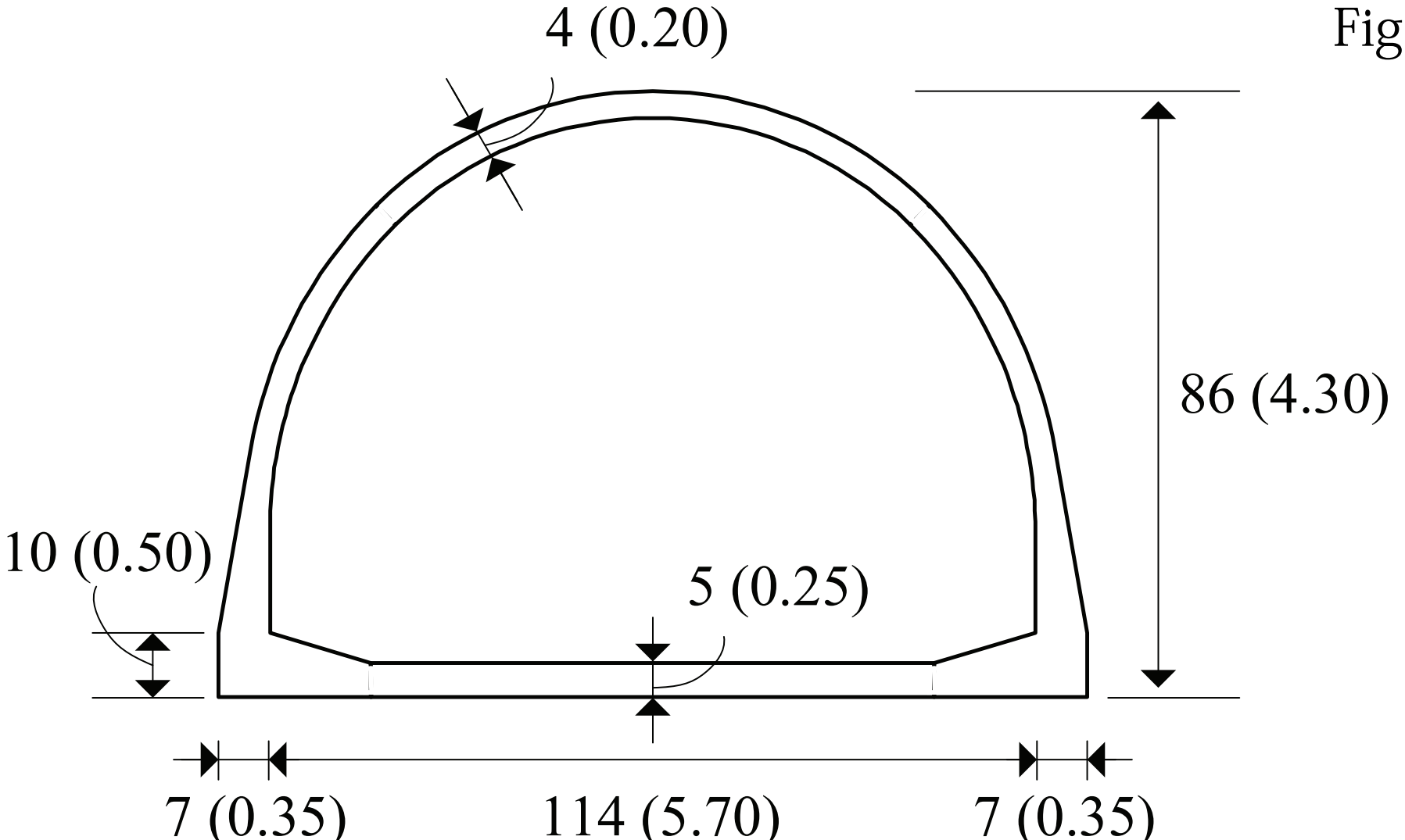

Unit: mm (in parenthesis, it is a prototype size)


(a)


(b)

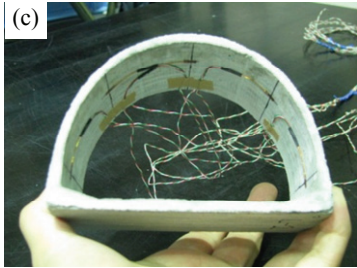
(c)

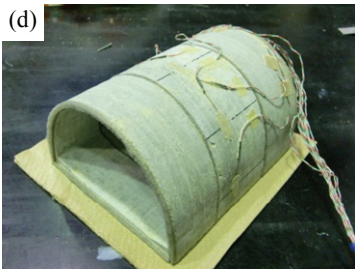
(d)


(e)

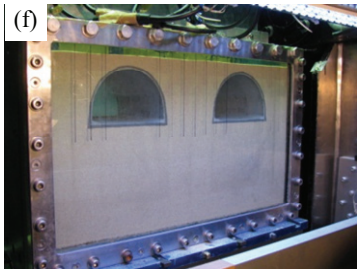
(f)

Fig. 5

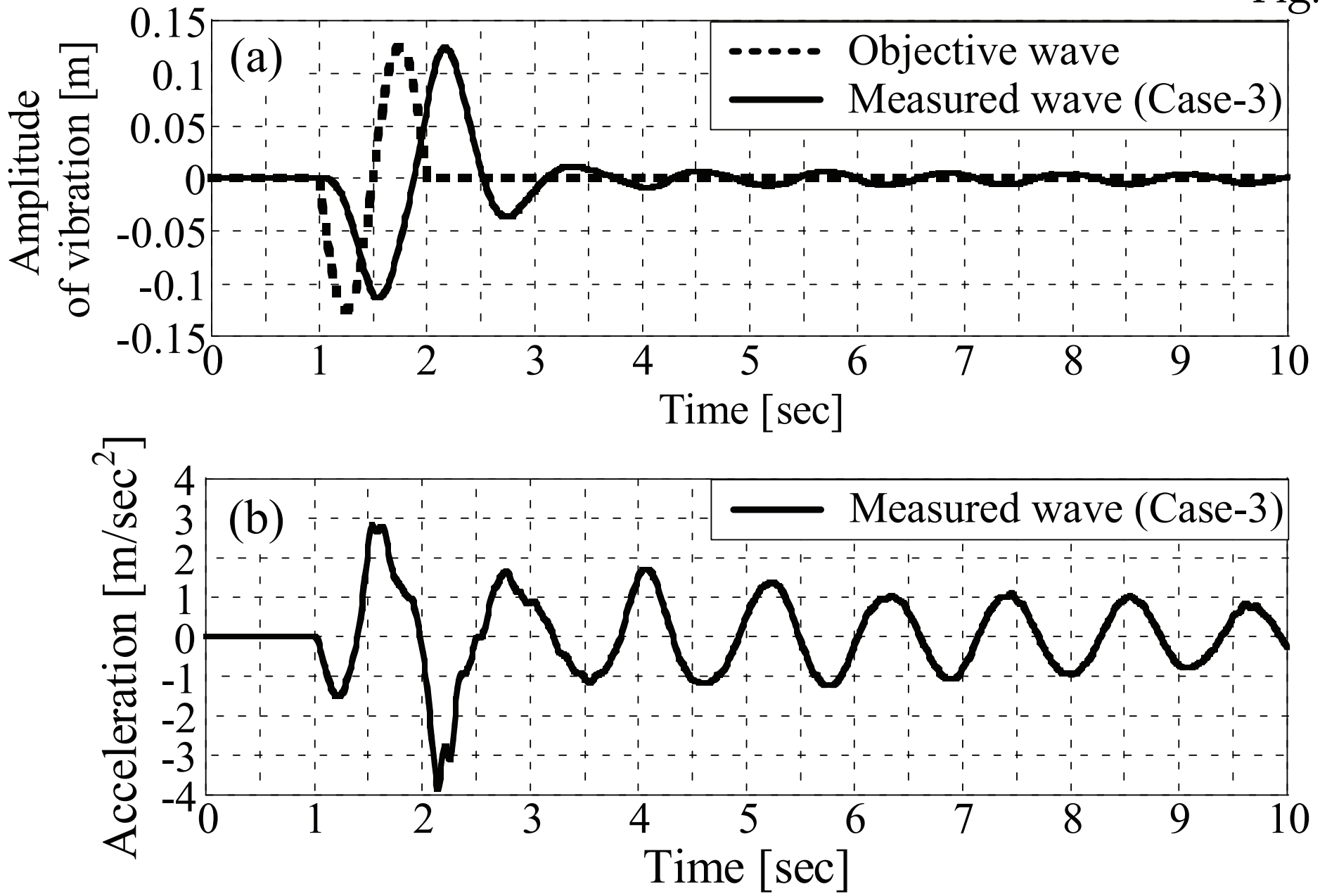
(a)
Objective wave
Measured wave (Case-3)
Amplitude of vibration [m]
0.15
0.1
0.05
0
-0.05
-0.1
-0.15
0
1
2
3
4
5
6
7
8
9
10
Time [sec]
(b)
Measured wave (Case-3)
Acceleration [m/sec^2]
4
3
2
1
0
-1
-2
-3
-4
0
1
2
3
4
5
6
7
8
9
10
Time [sec]

Fig. 6

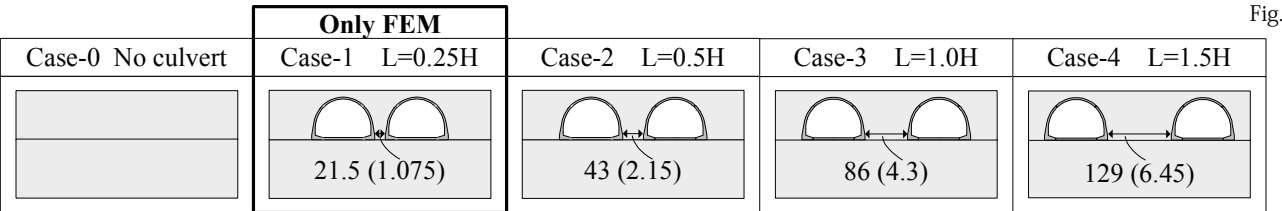

Unit: mm (in parenthesis, it is a prototype size)

Fig. 7

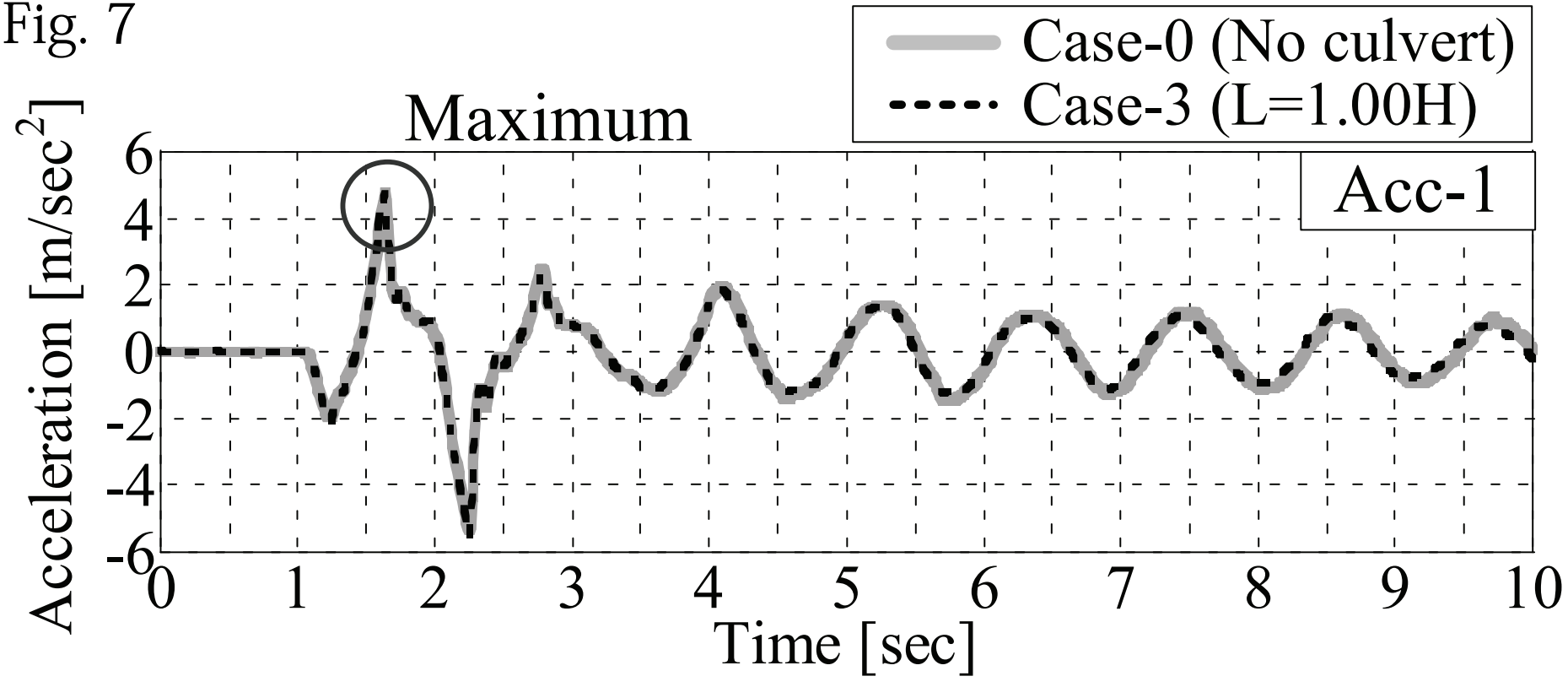
Case-0 (No culvert)
Case-3 (L=1.00H)
Maximum
Acc-1
Acceleration [m/sec^2]
6
4
2
0
-2
-4
-6
0
1
2
3
4
5
6
7
8
9
10
Time [sec]

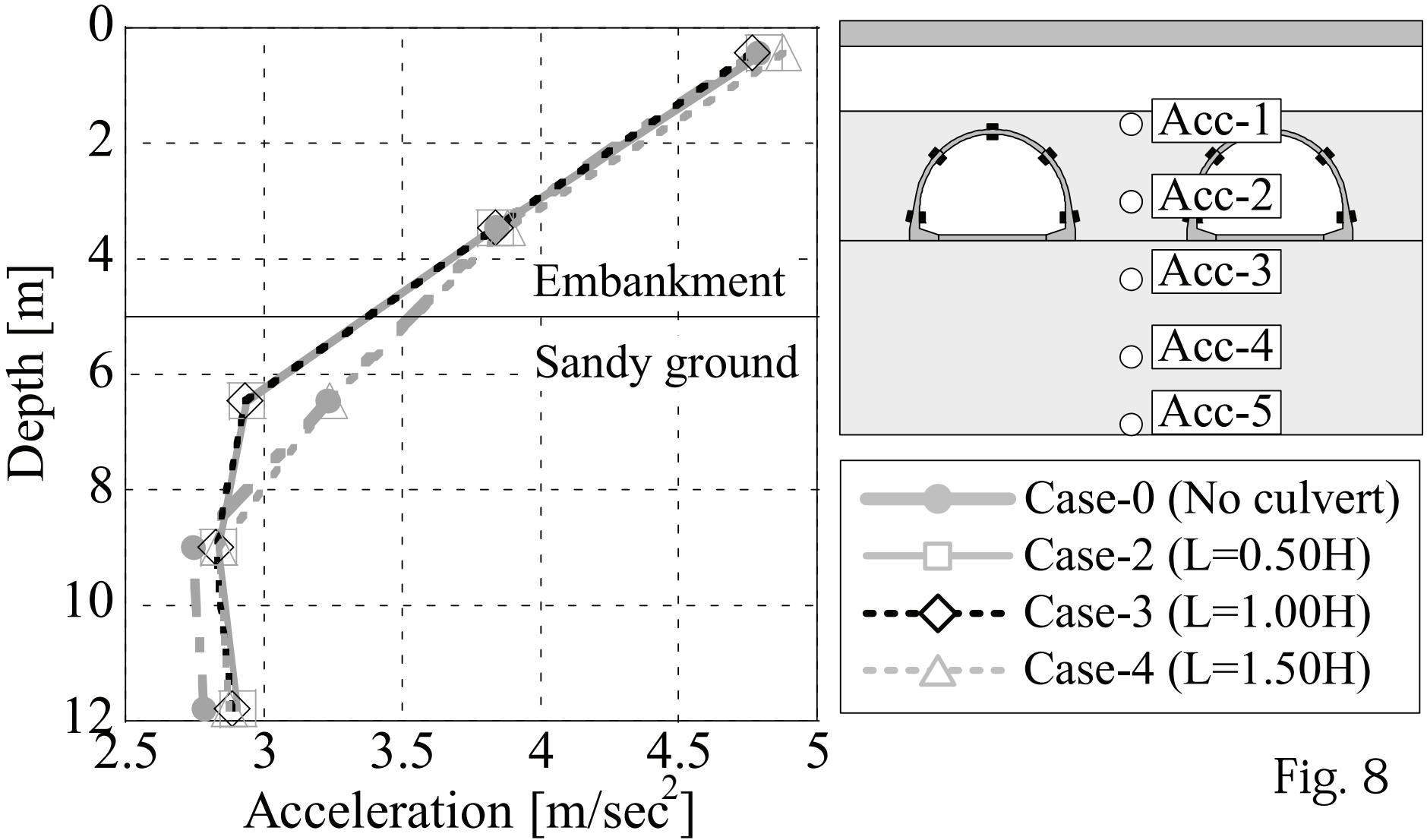
0
2
4
6
8
10
12
Depth [m]
Embankment
Sandy ground
2.5
3
3.5
4
4.5
5
Acceleration [m/sec2]
Acc-1
Acc-2
Acc-3
Acc-4
Acc-5
Case-0 (No culvert)
Case-2 (L=0.50H)
Case-3 (L=1.00H)
Case-4 (L=1.50H)

Fig. 8

Fig. 9

Unit: kN*m/m

(a)

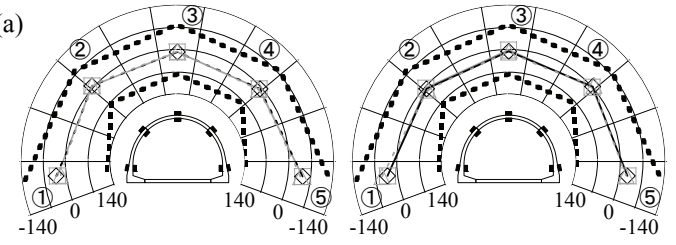

	Left-hand side culvert					Right-hand side culvert				
	①	②	③	④	⑤	①	②	③	④	⑤
Case-2	-27.2	-4.4	7.6	7.2	–44.9	-32.3	5.0	2.7	2.0	–26.1
Case-3	-32.9	-4.4	9.1	6.1	–46.1	-32.7	-6.8	5.3	–1.0	–23.6
Case-4	-17.4	-7.2	5.4	10.5	–39.3	-49.0	14.5	9.0	–7.7	–19.3

(b)

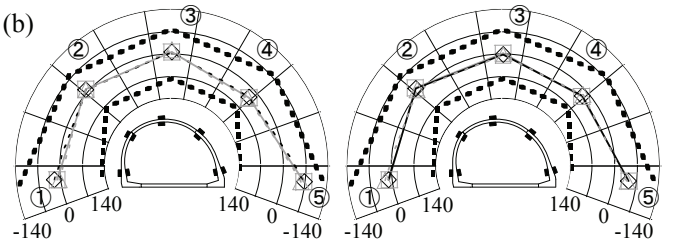

	Left-hand side culvert					Right-hand side culvert				
	①	②	③	④	⑤	①	②	③	④	⑤
Case-2	-10.2	-10.1	-6.6	28.2	–65.7	-8.5	-17.0	-6.6	28.2	–47.5
Case-3	-19.9	-8.3	-5.6	26.3	–67.4	-10.3	-15.2	3.0	18.9	–45.6
Case-4	-4.8	-9.1	-12.4	31.5	–57.6	-22.3	-8.9	3.6	15.3	–41.5

(c)

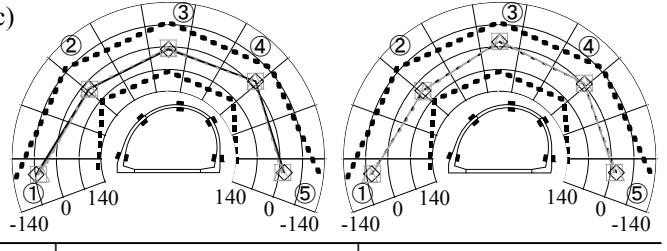

	Left-hand side culvert					Right-hand side culvert				
	①	②	③	④	⑤	①	②	③	④	⑤
Case-2	-58.7	22.1	3.4	–13.6	–12.4	-50.0	30.8	-15.5	–4.2	–12.7
Case-3	-65.0	20.2	7.9	–15.0	–15.4	-52.5	30.6	-15.2	–3.2	–17.1
Case-4	-49.6	17.8	5.3	–13.1	–7.6	-60.0	35.1	-17.4	–4.1	–17.6

(d)

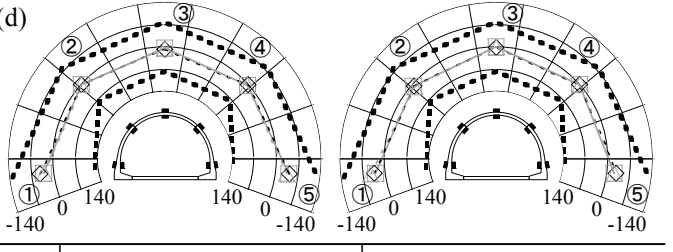

	Left-hand side culvert					Right-hand side culvert				
	①	②	③	④	⑤	①	②	③	④	⑤
Case-2	-32.6	1.6	5.2	3.6	–39.9	-30.8	6.7	0.0	1.9	–22.5
Case-3	-41.6	1.4	8.2	2.2	–43.2	-33.6	7.5	1.8	0.5	–28.4
Case-4	-29.6	1.2	3.9	4.6	–33.5	-44.1	11.9	2.7	–2.0	–22.8

NODE: 2490
ELEMENT: 2378

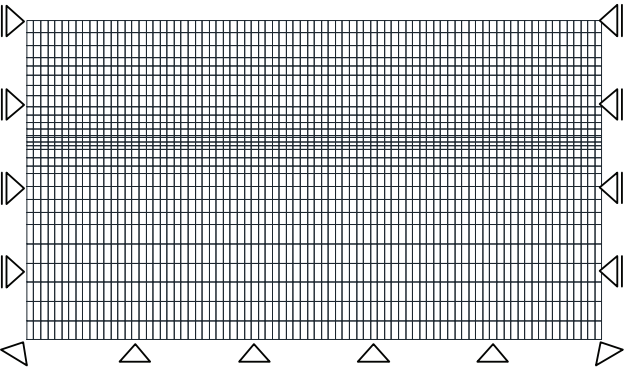

(a)

NODE: 2678
ELEMENT: 2384

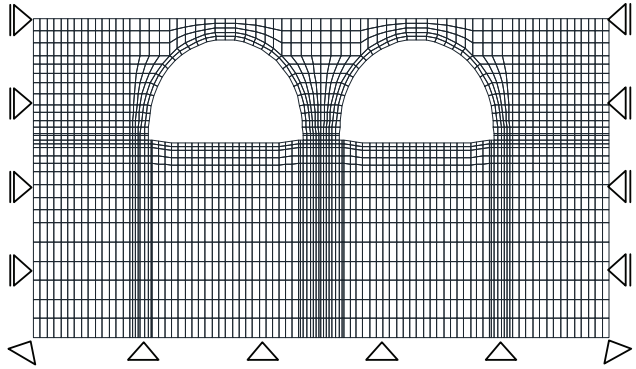

(b)

NODE: 2678
ELEMENT: 2384

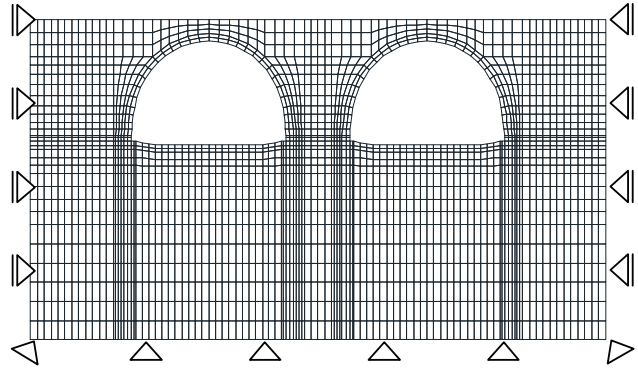

(c)

NODE: 2678
ELEMENT: 2384

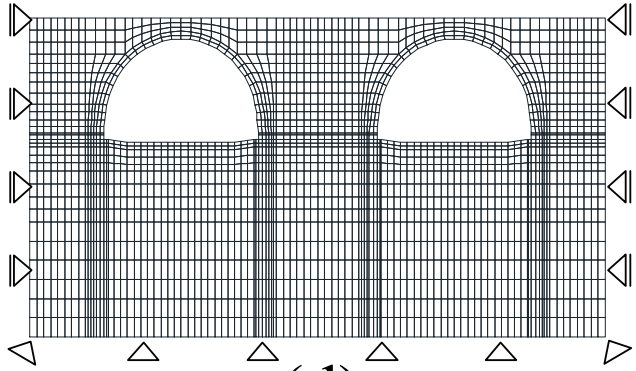

(d)

NODE: 2678
ELEMENT: 2384

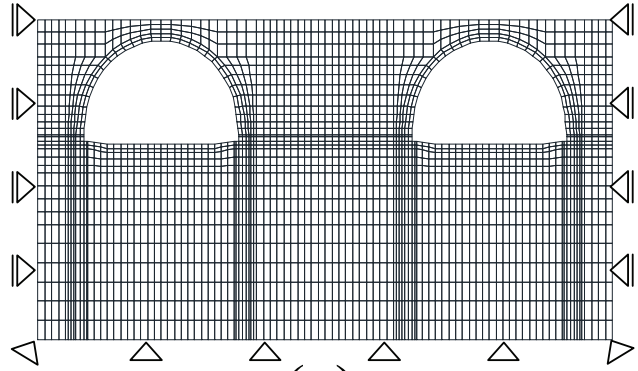

(e)

Fig. 10

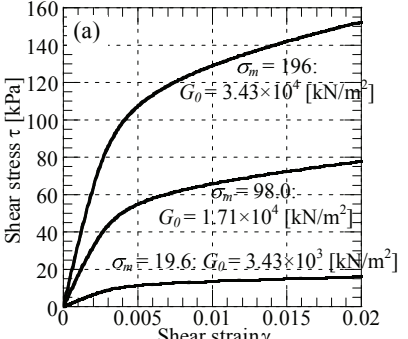
(a)
σ_m = 196:
G_0 = 3.43×10^4 [kN/m^2]
σ_m = 98.0:
G_0 = 1.71×10^4 [kN/m^2]
σ_m = 19.6: G_0 = 3.43×10^3 [kN/m^2]
Shear stress τ [kPa]
Shear strain γ
0
20
40
60
80
100
120
140
160
0.005
0.01
0.015
0.02

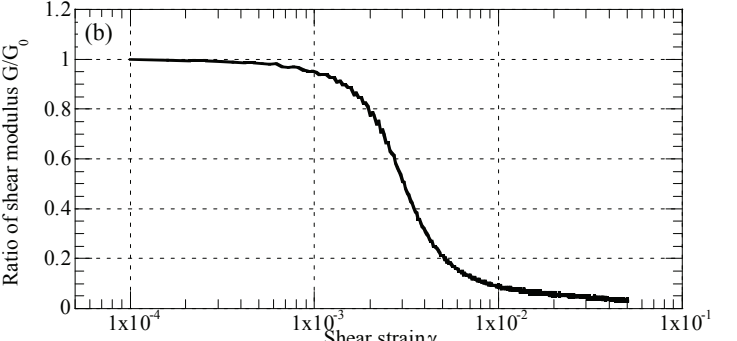
(b)
Ratio of shear modulus G/G$_0$
Shear strain γ
0
0.2
0.4
0.6
0.8
1
1.2
1x10^{-4}
1x10^{-3}
1x10^{-2}
1x10^{-1}

Fig. 12

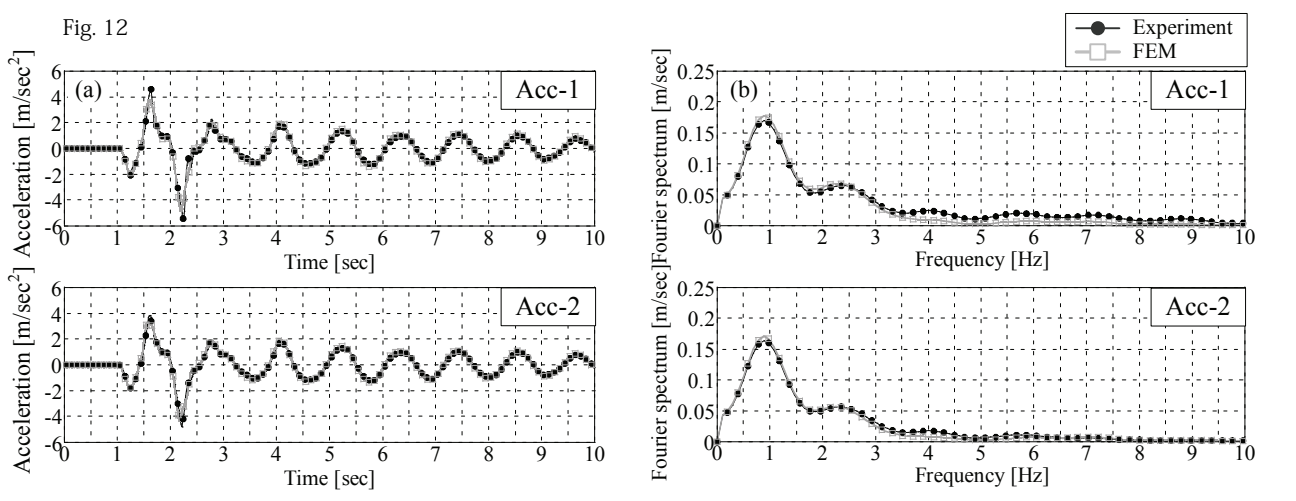
(a)
Acc-1
Acceleration [m/sec^2]
Time [sec]
Acc-2
Acceleration [m/sec^2]
Time [sec]
Experiment
FEM
(b)
Acc-1
Fourier spectrum [m/sec]
Frequency [Hz]
Acc-2
Fourier spectrum [m/sec]
Frequency [Hz]

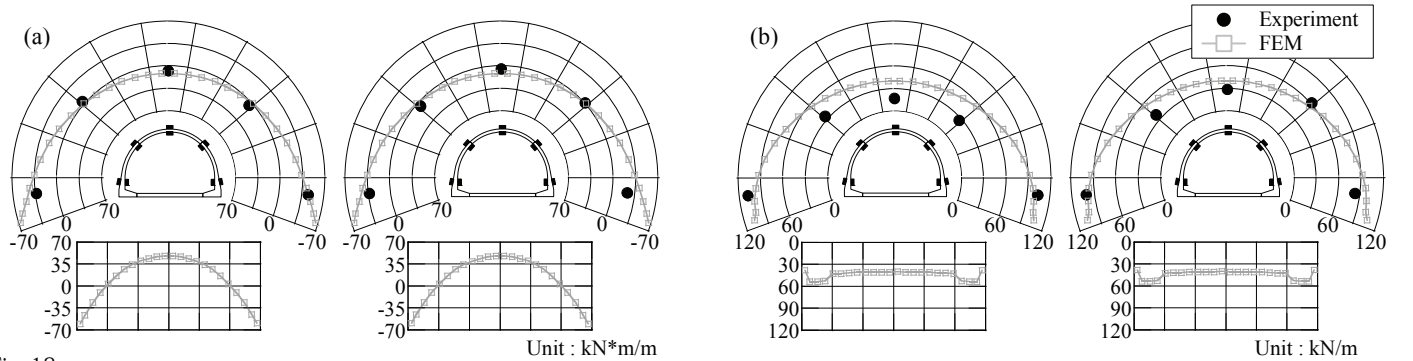

Fig. 13

Fig. 14

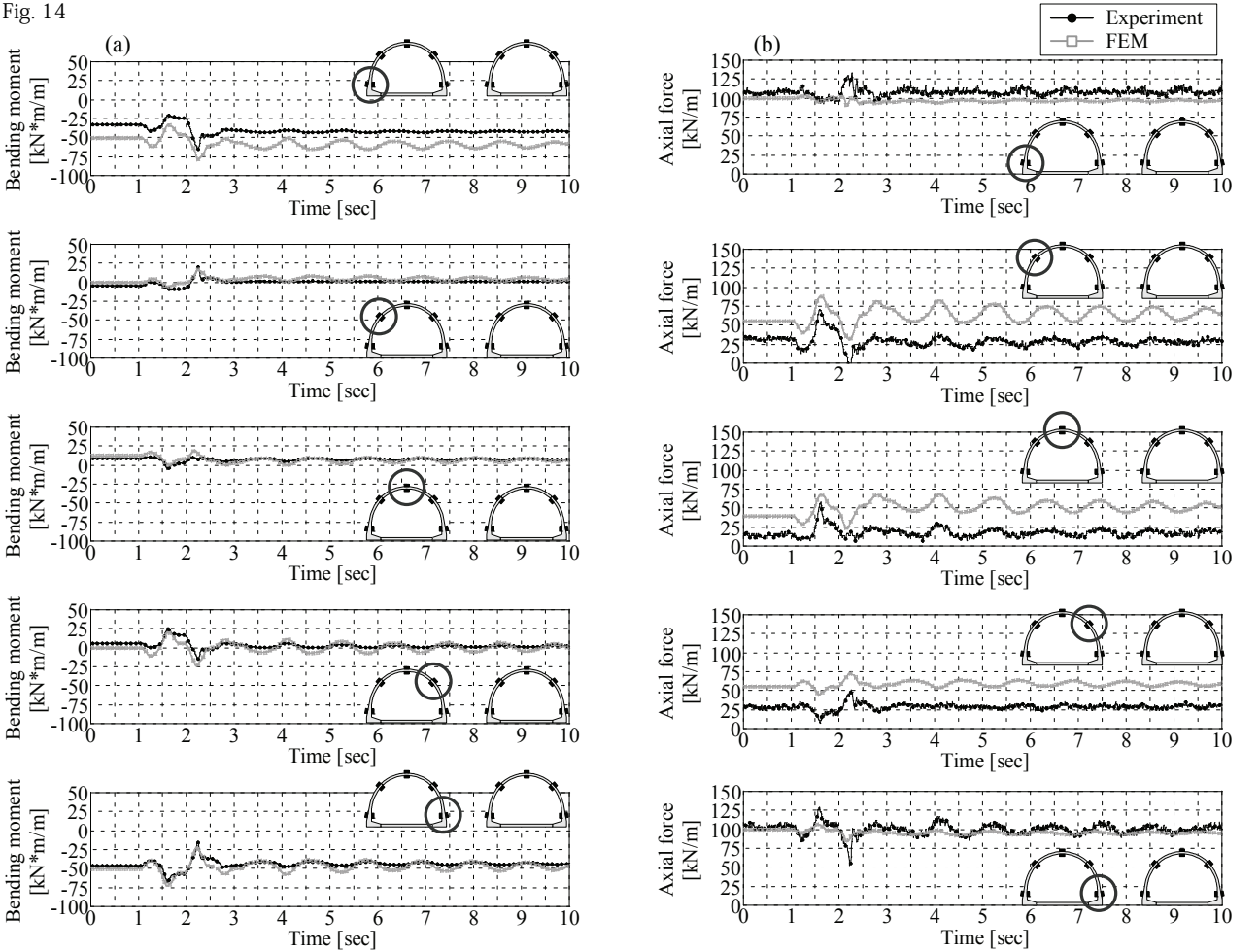
(a)
(b)
Experiment
FEM
Bending moment [kN*m/m]
Axial force [kN/m]
Time [sec]

Fig. 15

(a)

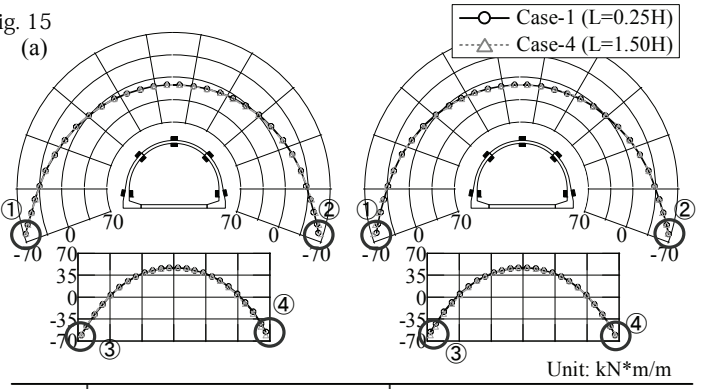

Unit: kN*m/m

	Left-hand side culvert				Right-hand side culvert			
	①	②	③	④	①	②	③	④
Case-1	-66.4	-61.7	-59.9	-55.0	-61.7	-66.4	-55.0	-59.9
Case-2	-66.3	-64.2	-59.7	-57.5	-64.2	-66.3	-57.5	-59.7
Case-3	-66.2	-66.2	-59.7	-59.5	-66.2	-66.2	-59.5	-59.7
Case-4	-65.6	-66.4	-58.9	-59.7	-66.4	-65.6	-59.7	-58.9

(b)

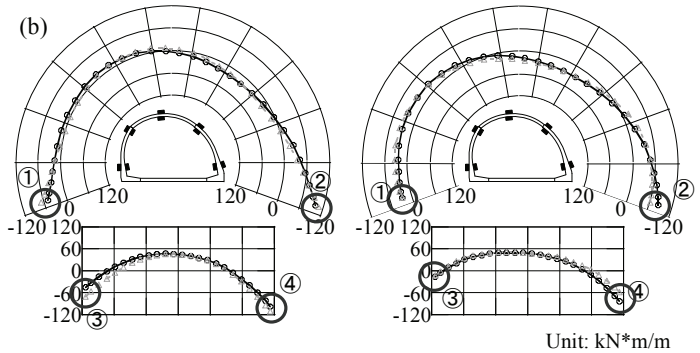

Unit: kN*m/m

	Left-hand side culvert				Right-hand side culvert			
	①	②	③	④	①	②	③	④
Case-1	-48.0	-99.9	-45.4	-97.8	-25.6	-91.2	-15.2	-83.0
Case-2	-51.3	-104.0	-49.7	-103.0	-26.7	-87.9	-15.3	-78.9
Case-3	-59.1	-107.6	-59.6	-108.5	-26.8	-79.5	-13.6	-69.5
Case-4	-66.7	-108.2	-70.0	-110.8	-26.9	-68.6	-12.2	-58.1

(c)

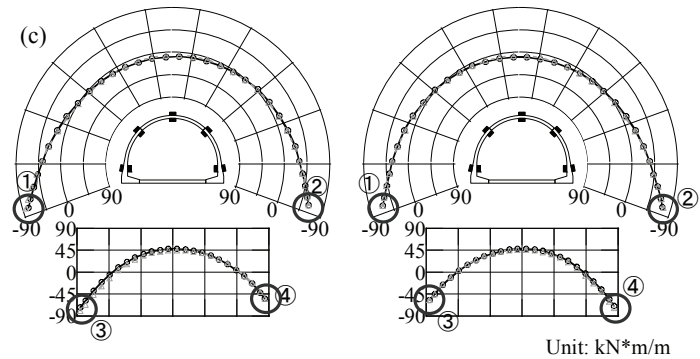

Unit: kN*m/m

	Left-hand side culvert				Right-hand side culvert			
	①	②	③	④	①	②	③	④
Case-1	-76.5	-60.5	-72.1	-54.5	-62.7	-73.8	-57.0	-69.1
Case-2	-77.0	-62.9	-73.0	-56.8	-65.1	-74.4	-59.3	-69.7
Case-3	-81.1	-63.5	-77.6	-57.3	-66.1	-75.7	-60.2	-71.7
Case-4	-82.6	-60.6	-79.5	-54.4	-63.6	-76.7	-57.7	-73.2

Fig. 16

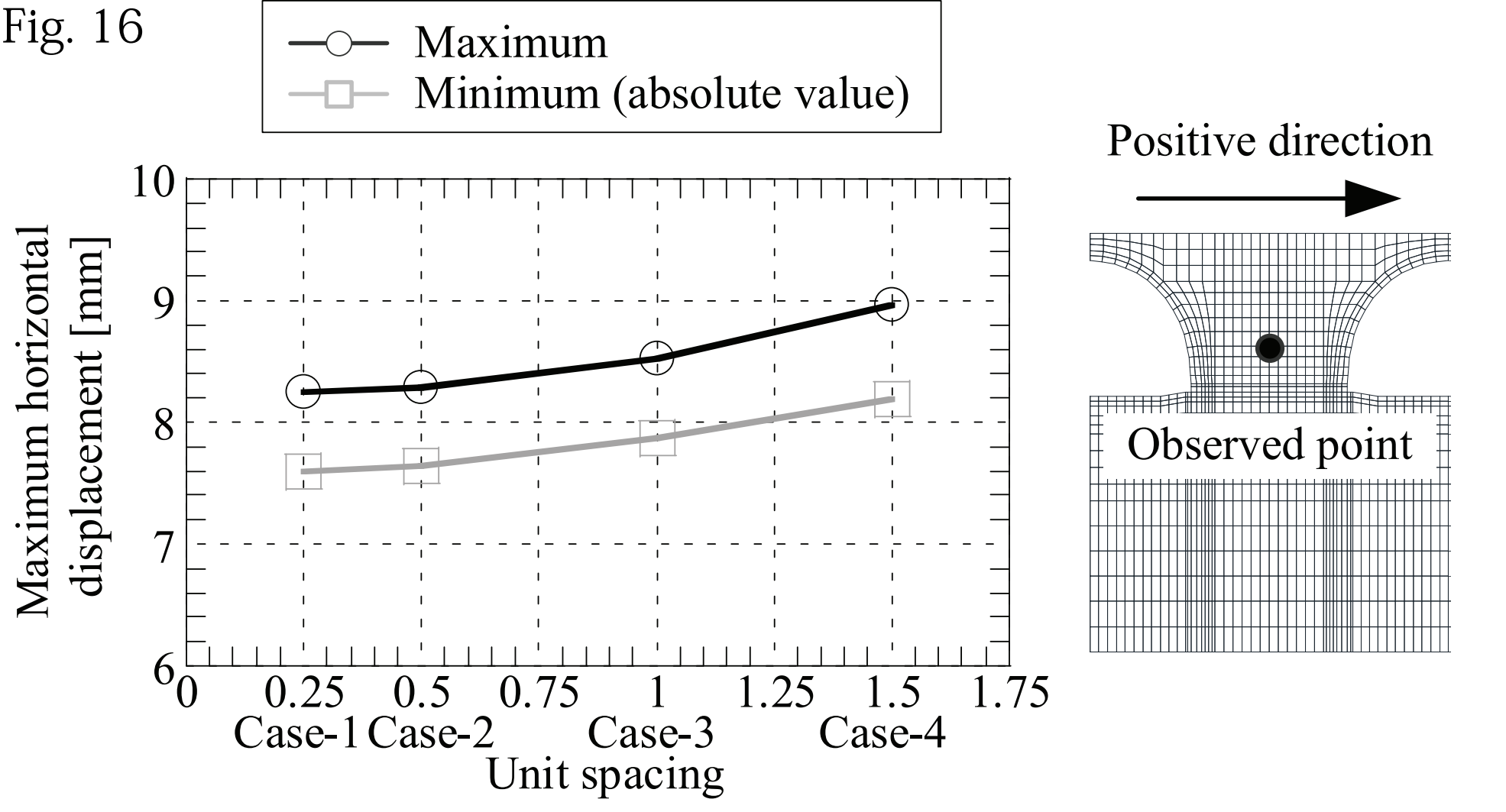
Maximum
Minimum (absolute value)
Maximum horizontal displacement [mm]
10
9
8
7
6
0
0.25
0.5
0.75
1
1.25
1.5
1.75
Case-1
Case-2
Case-3
Case-4
Unit spacing
Positive direction
Observed point

Fig. 17

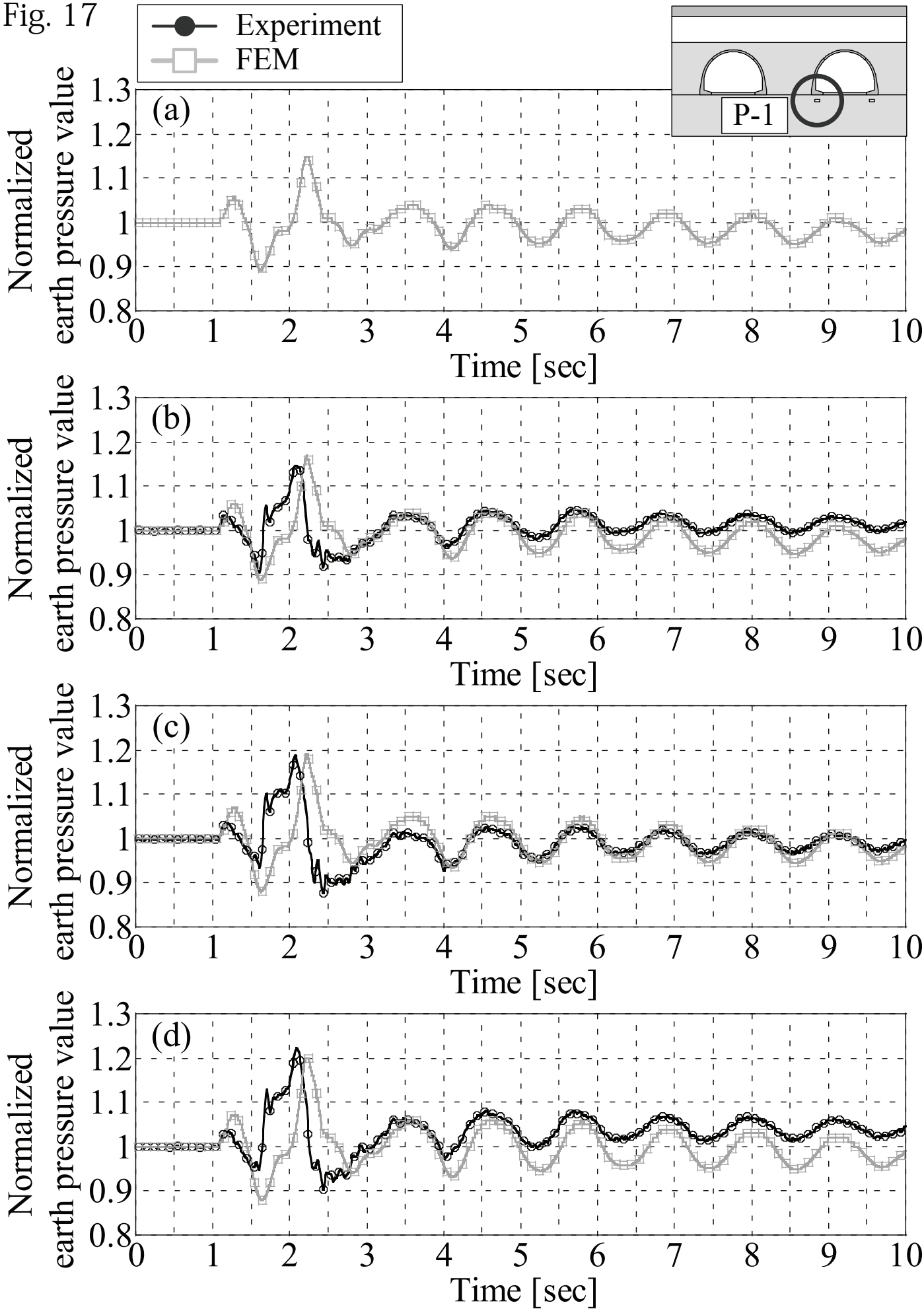
Experiment
FEM
P-1
(a)
(b)
(c)
(d)
Normalized earth pressure value
Time [sec]
1.3
1.2
1.1
1
0.9
0.8
0
1
2
3
4
5
6
7
8
9
10

Fig. 18

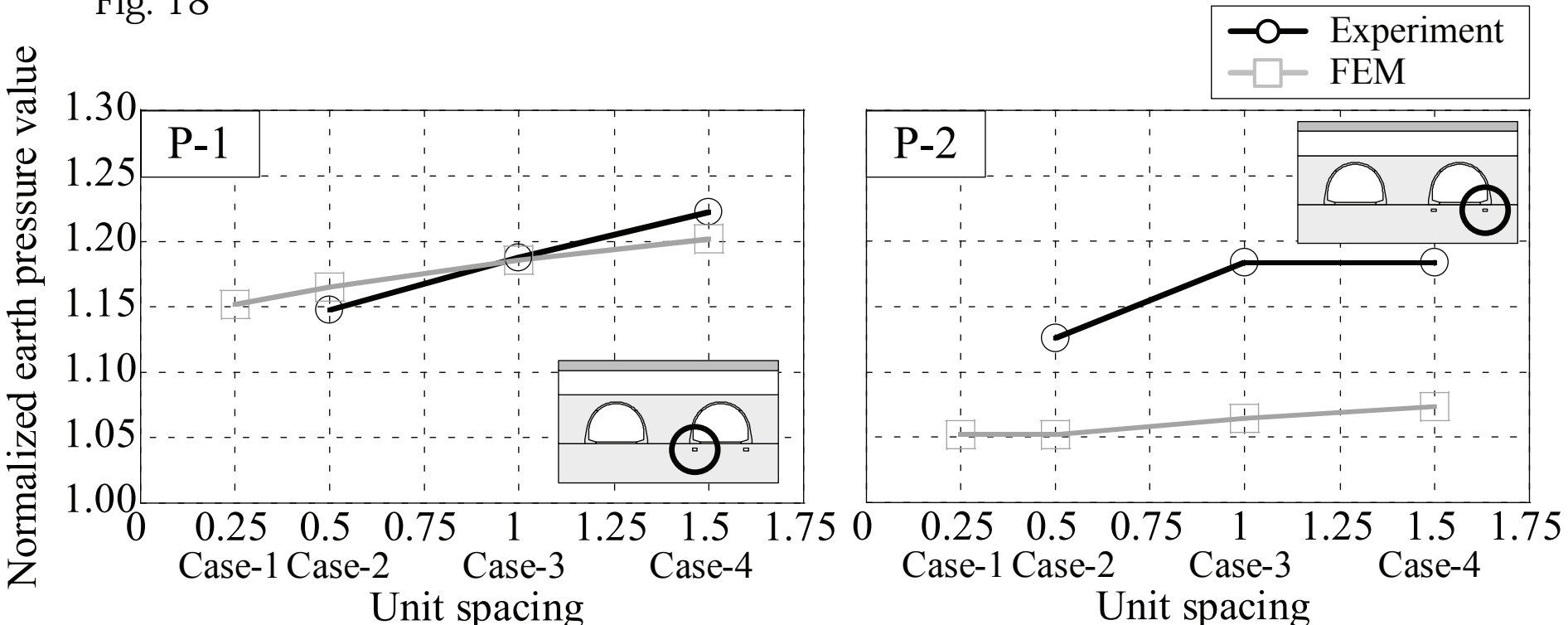
Experiment
FEM
P-1
P-2
Normalized earth pressure value
1.30
1.25
1.20
1.15
1.10
1.05
1.00
0
0.25
0.5
0.75
1
1.25
1.5
1.75
Case-1
Case-2
Case-3
Case-4
Unit spacing

Fig. 19

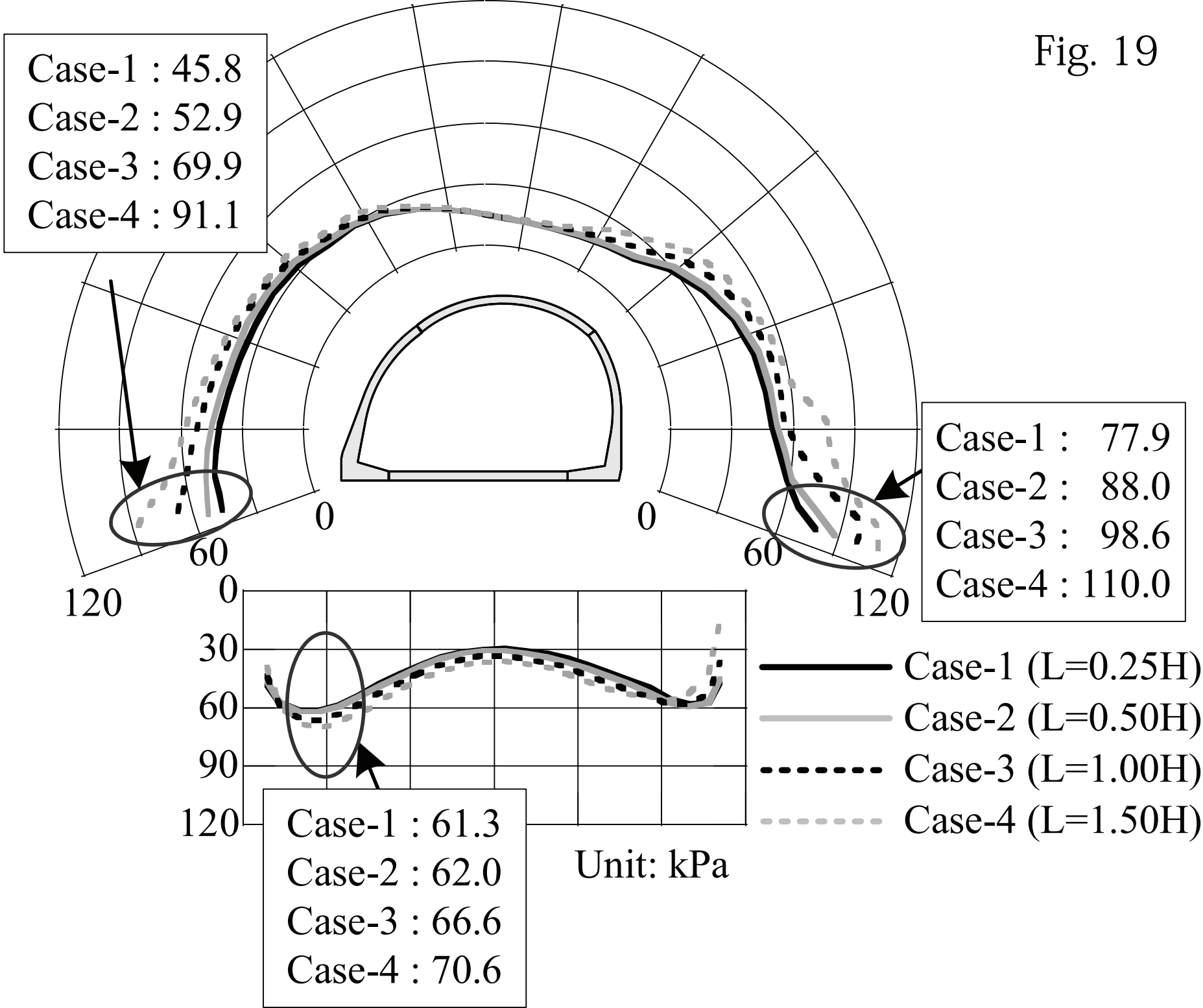
Case-1 : 45.8
Case-2 : 52.9
Case-3 : 69.9
Case-4 : 91.1
Case-1 : 77.9
Case-2 : 88.0
Case-3 : 98.6
Case-4 : 110.0
0
60
120
0
30
60
90
120
Case-1 : 61.3
Case-2 : 62.0
Case-3 : 66.6
Case-4 : 70.6
Unit: kPa
Case-1 (L=0.25H)
Case-2 (L=0.50H)
Case-3 (L=1.00H)
Case-4 (L=1.50H)

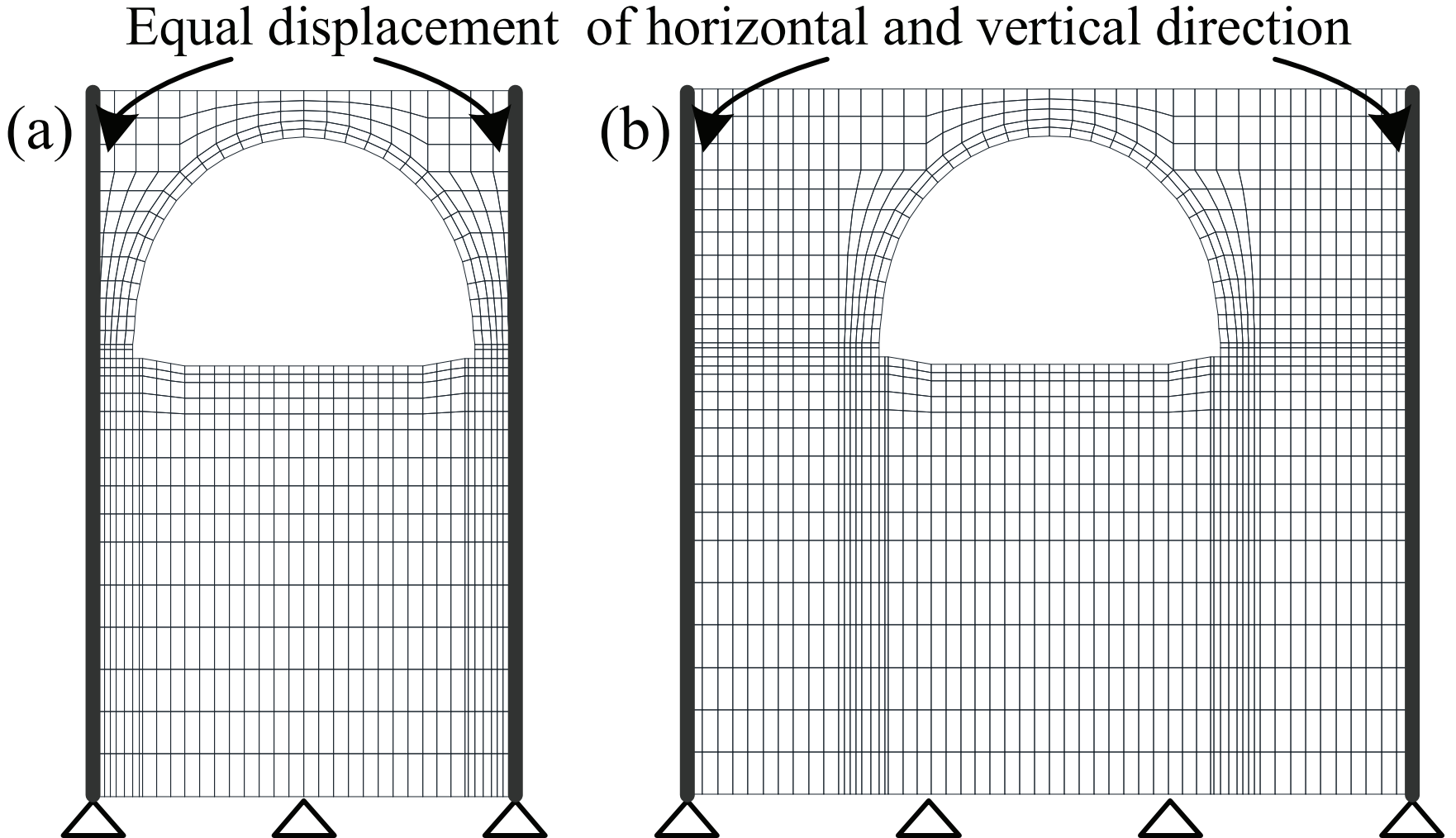
Equal displacement of horizontal and vertical direction
(a)
(b)

Fig. 21

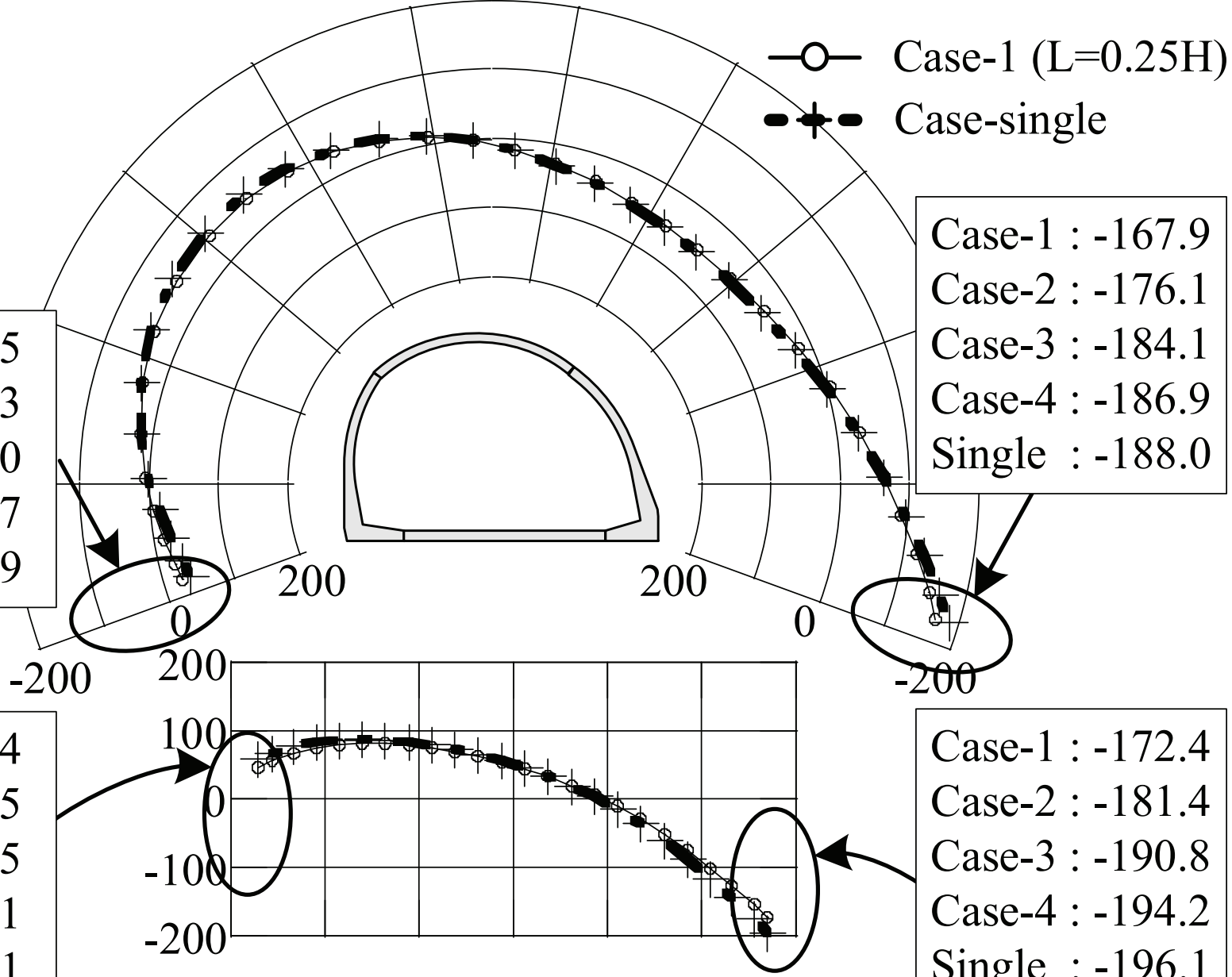

Unit: kN*m/m

Fig. 22

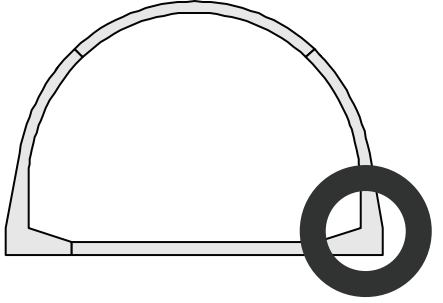

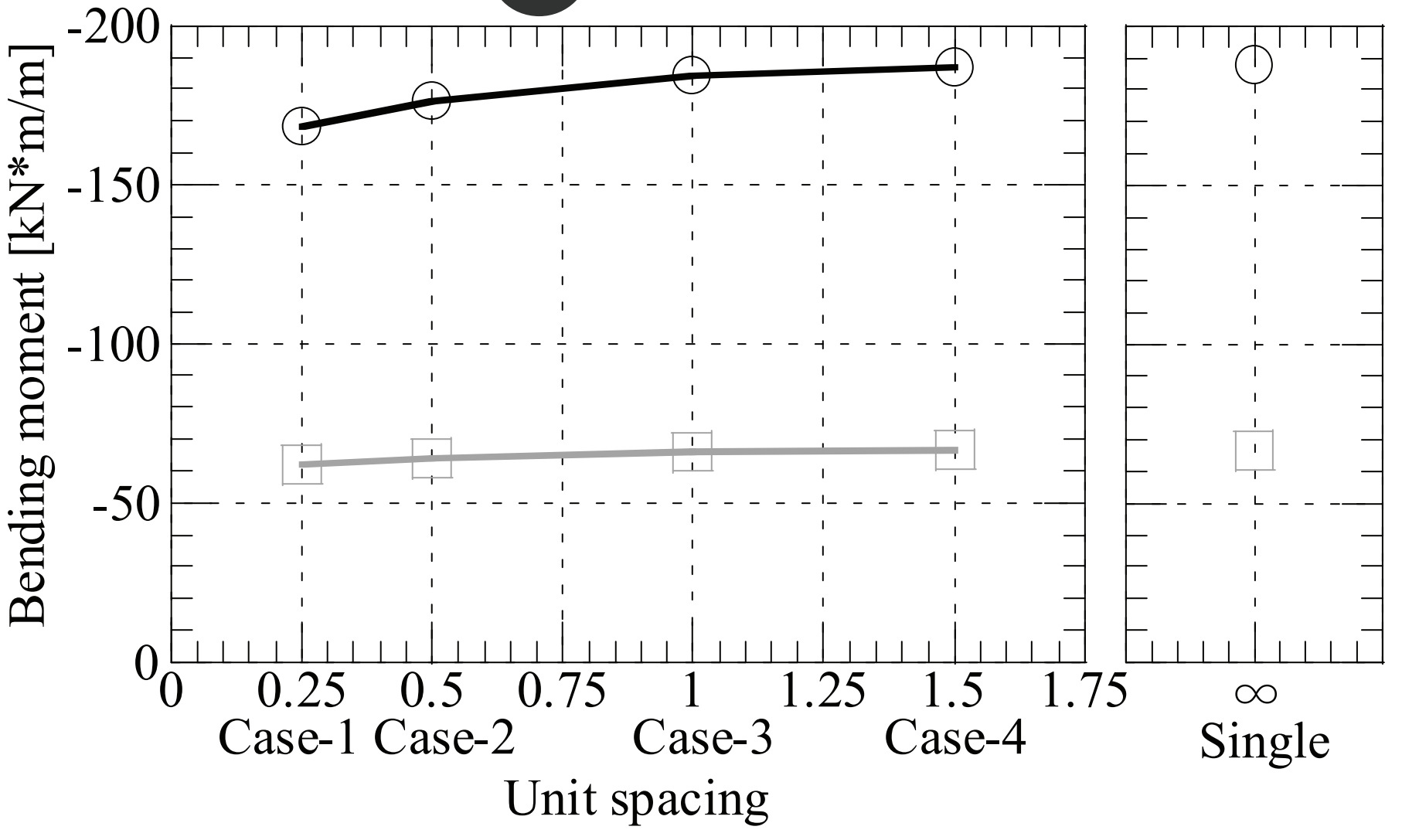
Maximum
Initial state
-200
-150
-100
-50
0
Bending moment [kN*m/m]
0
0.25
0.5
0.75
1
1.25
1.5
1.75
∞
Case-1
Case-2
Case-3
Case-4
Single
Unit spacing

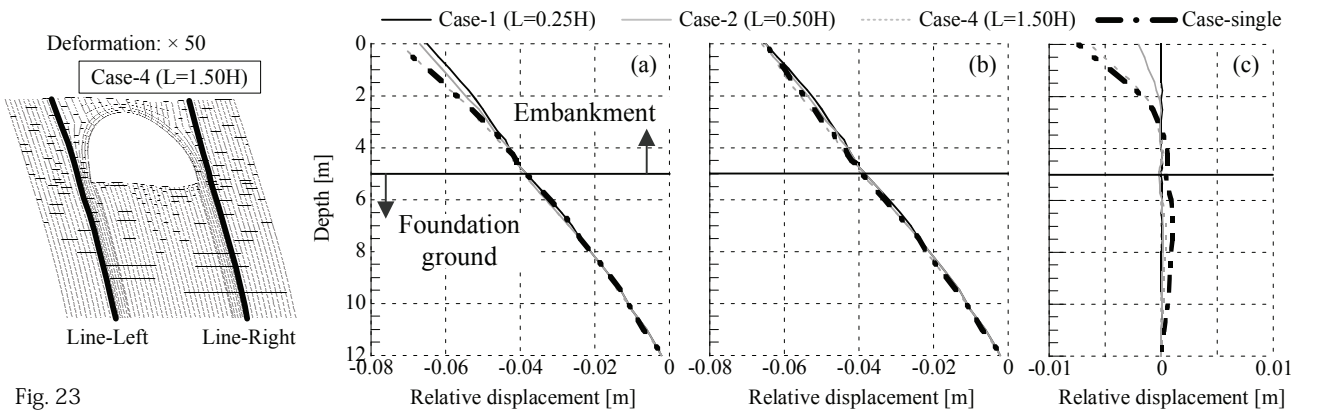
Deformation: × 50
Case-4 (L=1.50H)
Line-Left
Line-Right
Case-1 (L=0.25H)
Case-2 (L=0.50H)
Case-4 (L=1.50H)
Case-single
(a)
(b)
(c)
Embankment
Foundation ground
Depth [m]
0
2
4
6
8
10
12
-0.08
-0.06
-0.04
-0.02
0
-0.01
0.01
Relative displacement [m]
Relative displacement [m]
Relative displacement [m]

Fig. 23

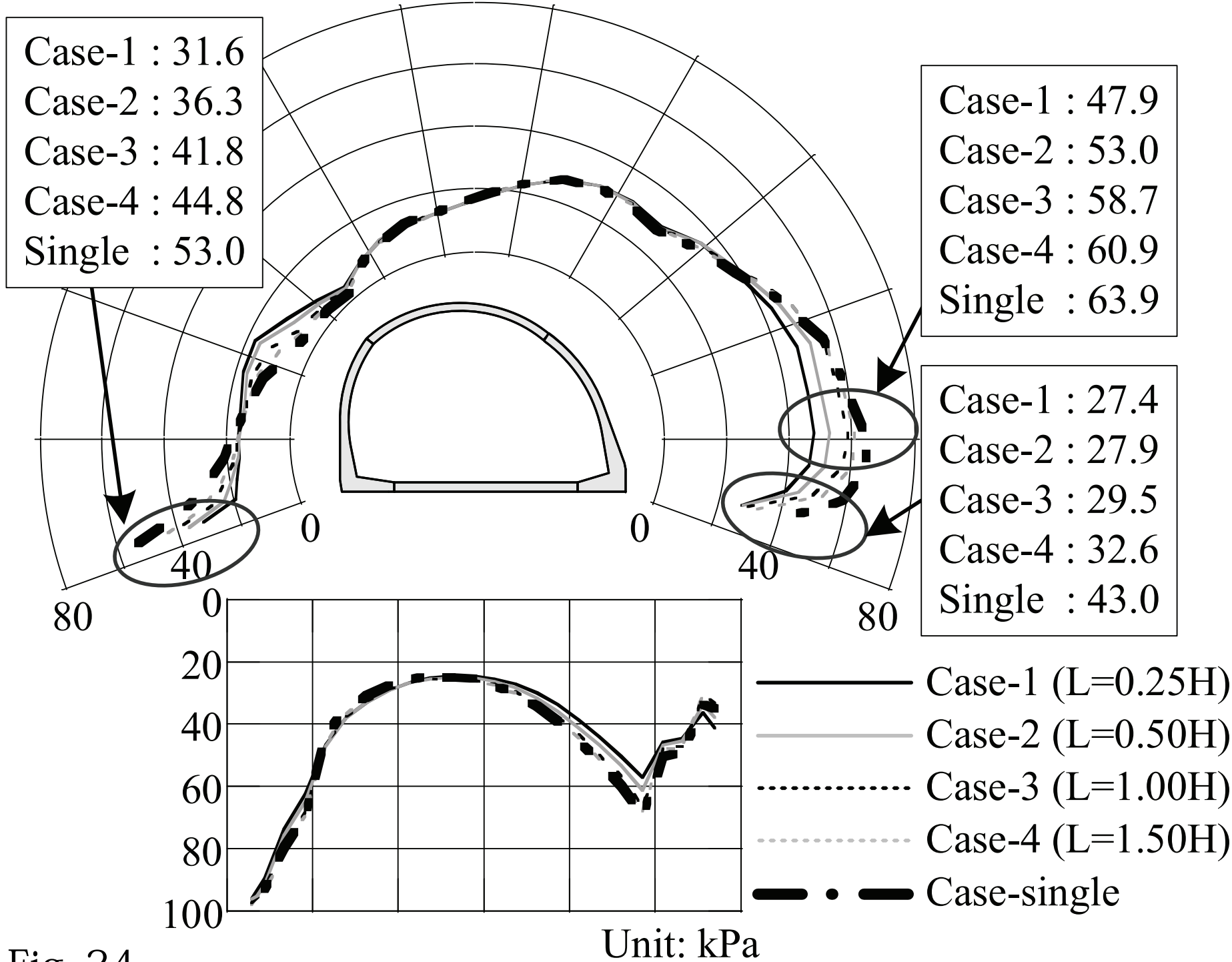
Case-1 : 31.6
Case-2 : 36.3
Case-3 : 41.8
Case-4 : 44.8
Single : 53.0
Case-1 : 47.9
Case-2 : 53.0
Case-3 : 58.7
Case-4 : 60.9
Single : 63.9
Case-1 : 27.4
Case-2 : 27.9
Case-3 : 29.5
Case-4 : 32.6
Single : 43.0
0
40
80
0
40
80
0
20
40
60
80
100
Case-1 (L=0.25H)
Case-2 (L=0.50H)
Case-3 (L=1.00H)
Case-4 (L=1.50H)
Case-single
Unit: kPa

Fig. 24

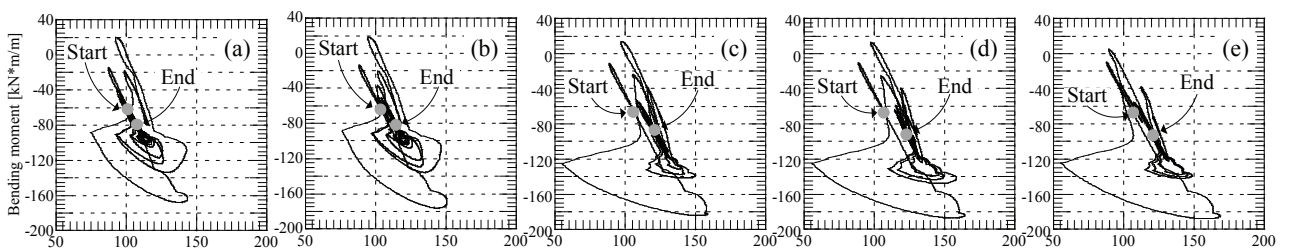
Start
End
(a)
(b)
(c)
(d)
(e)
Bending moment [kN*m/m]
Axial force [kN/m]
40
0
-40
-80
-120
-160
-200
50
100
150
200

Fig. 25

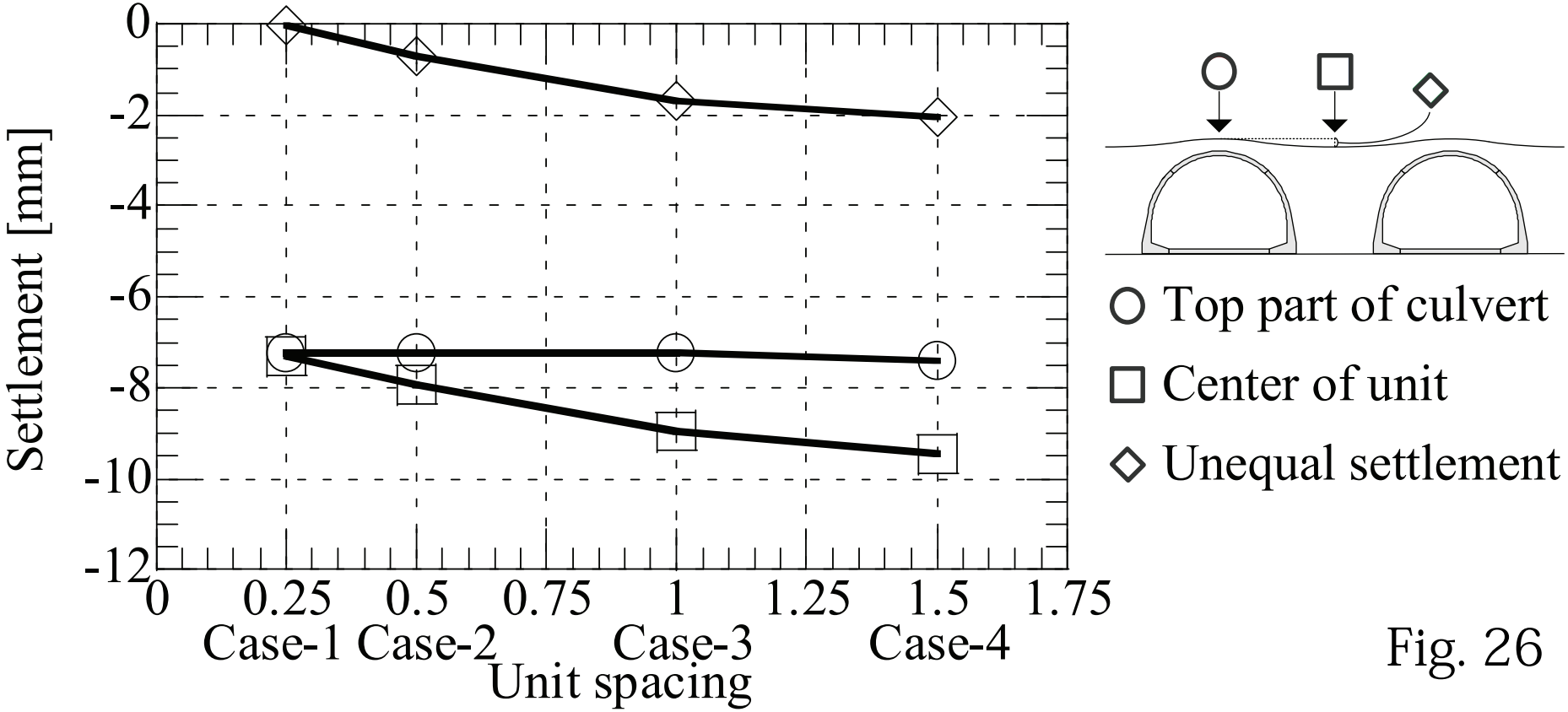
Settlement [mm]
0
-2
-4
-6
-8
-10
-12
0
0.25
0.5
0.75
1
1.25
1.5
1.75
Case-1
Case-2
Case-3
Case-4
Unit spacing
Top part of culvert
Center of unit
Unequal settlement

Fig. 26

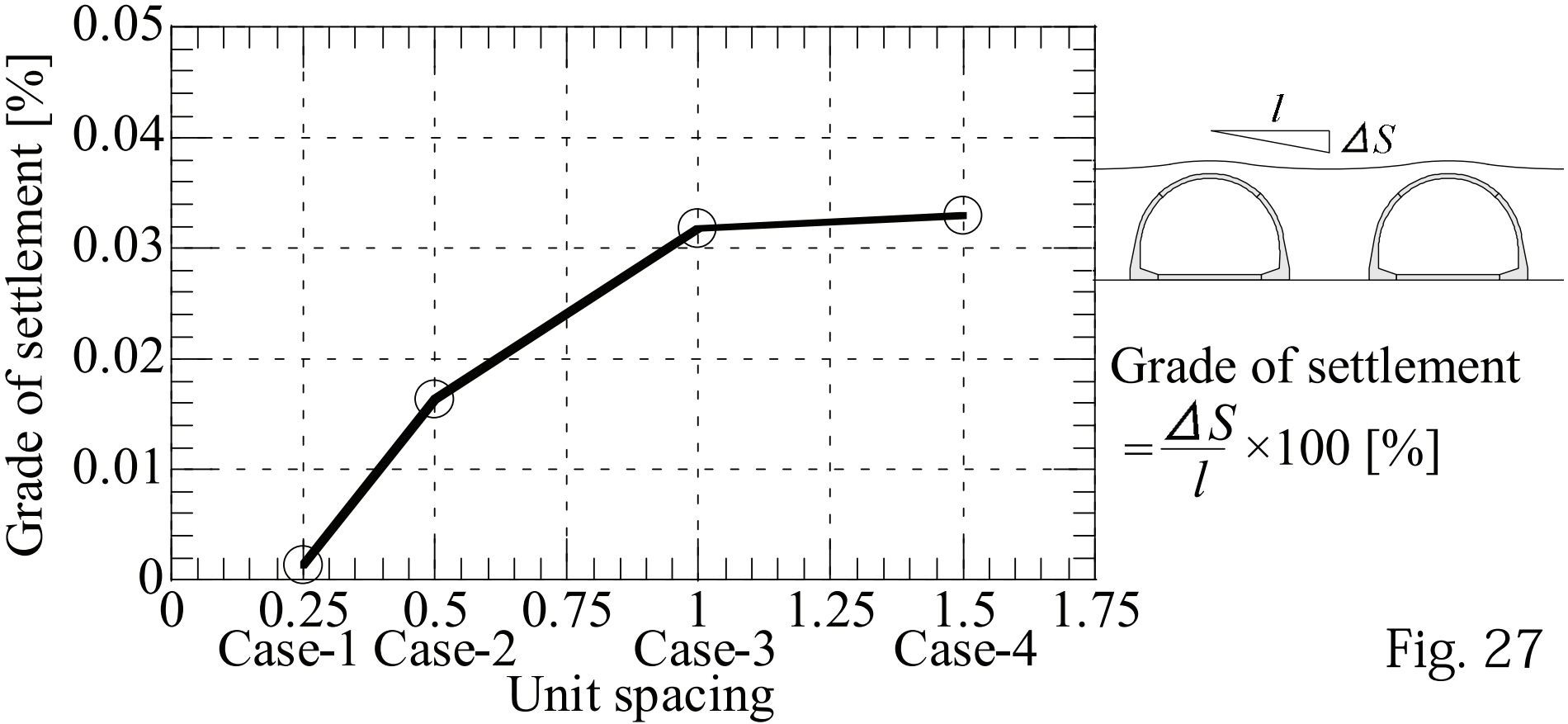
0.05
0.04
0.03
0.02
0.01
0
Grade of settlement [%]
0
0.25
0.5
0.75
1
1.25
1.5
1.75
Case-1
Case-2
Case-3
Case-4
Unit spacing
l
ΔS
Grade of settlement
$=\frac{\Delta S}{l}\times 100$ [%]

Fig. 27